Extracellular matrix proteins in hypoxia, 3D cancer spheroids as a model

Master's thesis
University of Turku
Department of Life Technologies
Molecular Systems Biology
December 2022

Ifrat Jahan Tamanna

The originality of this thesis has been checked in accordance with the University of Turku quality assurance system using the Turnitin Originality Check service.

UNIVERSITY OF TURKU
Department of Life Technologies
IFRAT JAHAN TAMANNA, Extracellular matrix proteins in hypoxia, 3D cancer spheroids as a model
Master's thesis, 74 p. Appendix, 4 p.
Molecular Systems biology
December 2022
The originality of this thesis has been checked in accordance with the University of Turku quality assurance system using the Turnitin Originality Check service.

The extracellular matrix (ECM) is a non-cellular network of cross-linked macromolecules, such as collagens, glycoproteins (fibronectin and laminins), and proteoglycans. The ECM plays a critical role in mediating cell adhesion, migration, differentiation, and proliferation. Thus, abnormal ECM remodeling can lead to pathological states and cancer metastasis. Fibroblasts, the most abundant cell type in the tumor stroma, produce several ECM components and proteins.

Hypoxia (low oxygen level) is a critical factor in cancer growth. The disruption in oxygen homeostasis leads to ECM remodeling. Therefore, many ECM proteins, such as collagens and laminins, are expressed differently. Increased deposition of these proteins can lead to ECM stiffness alterations, which can lead to cancer progression. 3D cell culture methods (spheroids) have gained increasing interest since they provide a more tissue-like environment compared to traditional 2D cell culture methods. We used 3D spheroids containing cancer cells and fibroblasts to mimic cutaneous squamous cell carcinoma (cSCC) tumors.

In this study, western blot results showed that in hypoxia, collagen prolyl hydroxylases (P4HA1 and P4HA2) and collagen lysyl hydroxylase (PLOD2) expression increased in both transformed keratinocytes and metastatic cSCC cells when they were cocultured with human primary skin fibroblasts. Laminin-332 expression was, however, downregulated. Immunofluorescence staining confirmed that P4HA1 expression was upregulated in 3D spheroids in hypoxic conditions. Proliferation assay showed that cell proliferation increased in hypoxia in mono- and cocultured spheroids. Mass spectrometry experiments also revealed different ECM protein expressions in hypoxia compared to normoxia. These results show that 3D spheroids containing cancer cells and fibroblasts are an indispensable tool for detecting ECM alterations in hypoxic conditions.

Keywords: ECM proteins, Hypoxia, Cancer 3D spheroid, Collagen, Laminin-332

Dedication

I would like to dedicate this project to my daughter, my beloved Mom, and my late Dad. Ammu and Abbu, without your incredible guidelines throughout my life, I could not be the person, I am today.
Shairah, my lovely daughter, without your support and sacrifice, completing this thesis would not be possible.
Love from deep of my heart.

ACKNOWLEDGEMENTS

I express my indebtedness, and sincere appreciation to Dr. Elina Siljamäki, Ph.D., Senior Researcher, Department of Life Technologies, University of Turku, Finland, for her constant supervision, important suggestions, and scholastic guidance in conducting the research and writing this manuscript.

I express my gratitude, gratefulness, and respect to my research co-supervisor and group leader of the Integrins research group, Dr. Jyrki Heino MD, Ph.D., Professor, Department of Life Technologies, University of Turku, Finland, for his kind cooperation, most beneficial advice, and factual comments during the research work and writing this manuscript.

Cordial thanks to my lab project supervisor Dr. Johanna Jokinen, Ph.D. teacher of, department of Life Technologies, and Dr. Pekka Rappu, Ph.D., Adjunct Professor of the Department of Life Technologies for all your support and guidelines during my project work and thesis. I would like to thank to my all-Integrin group members and lab fellows for your inspiration, continuous help, and kind co-operation during the period of thesis work.

Great thanks to Dr. Paula Mulo, Ph.D., Professor, Department of Life Technologies, and all my respective faculty members for delivering cutting-edge lectures during the study period. Thanks to all my friends.

Finally, I acknowledge my gratitude and profound respect to my beloved parents, elder sisters, and husband for their blessings and inspiration. Finally, I would like to thank my daughter for helping her mom this whole journey.

Ifrat Jahan Tamanna
Turku, 2022

Contents

ABBREVIATIONS

Abbreviation	**Full name**
ACN	Acetonitrile
APS	Ammonium persulfate
BCA	Bicinchoninic acid
BM	Basement membrane
BSA	Bovine serum albumin
COL	Collagen
cSCC	Cutaneous squamous cell carcinoma
DMEM	Dulbecco's modified eagle medium
DMSO	Dimethyl sulfoxide
DNA	Deoxyribonucleic acid
DTT	Dithiothreitol
ECM	Extracellular matrix
EDTA	Ethylenediaminetetraacetic acid
EGFR	Epidermal growth factor receptor
ERK	Extracellular signal-regulated kinase
FCS	Fetal calf serum
FGF	Fibroblast growth factor
GF	Growth factor
HCl	Hydrochloric acid
HIF-1	Hypoxia-inducible factor-1
IAA	Iodoacetamide
IF	Immunofluorescence
IL	Interleukin
MAPK	Mitogen-activated protein kinase
MMP	Matrix metalloproteinase
MMP9	Matrix metalloproteinase 9
MS	Mass spectrometry
NaCl	Sodium chloride
NEAA	Non-essential amino acid

P4HA1	Prolyl 4-hydroxylase subunit α−1
PAGE	Polyacrylamide gel electrophoresis
PBS	Phosphate-buffered saline
PBST	Phosphate-buffered saline with Tween-20
PDK1	Phosphoinositide dependent protein kinase 1
PFA	Paraformaldehyde
PHDs	Prolyl hydroxylase domain-containing proteins
PLOD2	Procollagen-lysine, 2-oxoglutarate 5-dioxygenase 2
PTM	Post-translational modification
p-CREB	Phosphorylated cAMP response element binding protein
p-ERK	Phosphorylated extracellular signal-regulated kinase
pVHL	Von Hippel-Lindau tumor suppressor
RIPA	Radio immunoprecipitation assay buffer
RT3	H-Ras-transformed keratinocytes
SD	Standard deviation
SDS-PAGE	Sodium dodecyl sulphate polyacrylamide gel electrophoresis
S. E. M	Standard error of the mean
TBST	Tris-buffered saline with Tween-20
TEMED	Tetramethylethylenediamine
TFA	Trifluoroacetic acid
TME	Tumor microenvironment
UT-SCC-7	University of Turku-Squamous Cell Carcinoma-7
w/v	Weight per volume
2D	Two dimensional
3D	Three dimensional

1. INTRODUCTION

1.1 Extracellular matrix

The extracellular matrix (ECM) is a highly dynamic and non-cellular compartment comprised of intercellular places. The ECM consists of cross-linked macromolecule network of collagens, glycoproteins (fibronectin and laminins), and proteoglycans. Although ECM is primarily a non-cellular space, it regulates most cellular activities through bioactive signaling molecules (Clause & Barker, 2013). It has a dynamic structure and network and it goes through remarkable changes and degradation from the developmental stage to the maturity level to maintain tissue homeostasis (Cox & Erler, 2011).

Cells generally require ECM to attach, grow, and differentiate. In this environment, ECM supports cells and anchorage the cell shape. It provides biochemical and mechanical support for tissues by regulating cell behavior, proliferation, migration, and invasion. ECM components and their subtypes regulate the functions and overall structure. Moreover, these components and their subtype activities and functions are necessary for body function (Walker et al., 2018). Conversely, in adverse conditions, matrix-degrading enzymes and dysregulation of the ECM are affiliated with different physiological and pathological conditions, such as cancer (Lu et al., 2011).

1.2 Principal components of the ECM

ECM is a complex network composed of three essential macromolecules: collagen, fibronectin, and glycoproteins like laminins. ECM also consists of adhesion molecules such as the integrin family, a transmembrane glycoprotein signaling family that attaches cells to the ECM by binding to various ECM and cell surface ligands (Bachmann et al., 2019). These ECM components are universal in almost all tissue types. However, tissue development differentiates ECM components in differential tissues (Schlie-Wolter et al., 2013). In addition, all these components have specific functions in the specialized cellular mechanisms. For example, cell adhesion, proliferation, and differentiation are mediated by cells binding to collagen, laminins, and fibronectin.

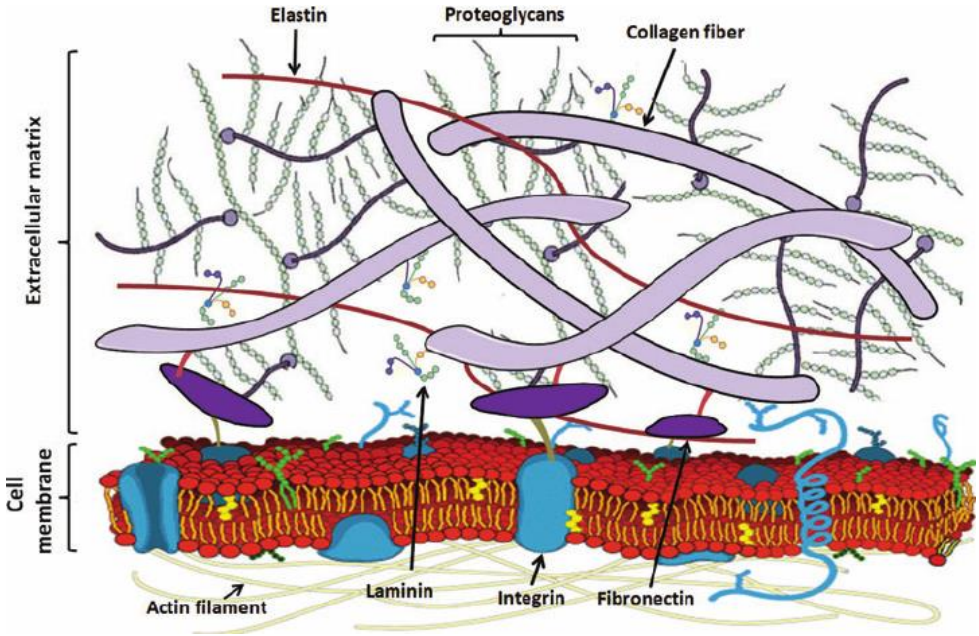

Figure 1. Significant components of the ECM. Its structure and the interaction between the components are simplified. The most abundant component of the ECM is collagen fiber. Also, proteoglycans, glycoproteins, laminins, and integrins have important functions in the ECM regulation and cell-to-cell and cell-to-ECM interaction. Picture from Xue *et al*., 2015.

1.3 Collagen, the basic structure of the ECM

Collagen is the most abundant fibrous protein and structural element in the ECM. In human, collagen accounts for 30% of the total proteins (Xu et al., 2019). Collagen affects the structure, shape, and mechanical organization of tissues. To date, twenty-eight types of collagens have been identified. All of them contain at least one triple-helical domain. This standard feature is present in collagen at different levels, from 10% to 96% (Ricard-Blum, 2011). Collagens interact with the cells with various receptors-like Integrin, Receptor Tyrosine Kinases (DDR), fibronectin and mediate several cellular activities, such as cell proliferation, differentiation, and migration (Elango et al., 2022). Different types of collagens have different functions. For example, collagen type IV mediates cell adhesion and division. It is also scaffolding other proteins like laminins and growth factor TGF-β (Khoshnoodi et al., 2008). Collagen VII functions as anchoring fibrils (Burgeson, 1993).

Collagen is rich in proline and glycine that are essential for collagen triple helix formation, and co-and post-translationally hydroxylated proline (Jaakkola et al., 2001). The stability of the triple helix structure is disrupted by enzymes like collagen prolyl hydroxylases (P4Hs) and lysyl hydroxylases, PLODs (Martins et al., 2020). These enzymes also play an essential role in cancer metastasis by accumulating and stiffening collagen in ECM (Gilkes et al., 2013a). In addition, collagen modulates tumor tissue stiffness and regulation of tumor immunity.

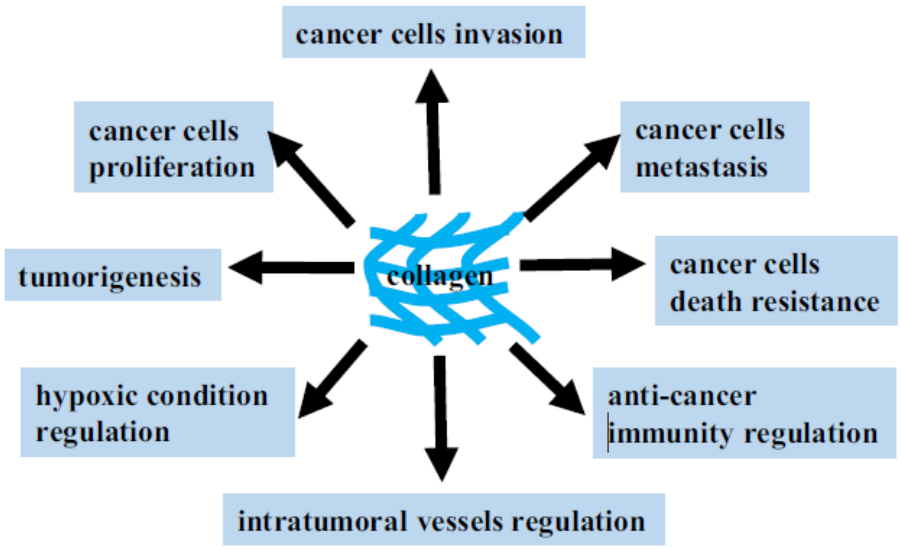

Figure 2. Collagen function in cancer. Collagen has various functions in cancer. Some crucial functions are cancer cell invasion, metastasis, hypoxic condition regulation, and anti-cancer immunity. Picture from Xu *et al*., 2019.

1.3.1 Collagen prolyl hydroxylase (P4H)

Prolyl hydroxylation is a common post-translational modification (PTM) that regulates protein folding and conformational stability. This post-translational modification is critical for the collagen triple helix stability (Jaakkola et al., 2001). Collagen contains a considerable amount of hydroxyproline, almost 4% in animal proteins. Collagen prolyl 4-hydroxylase (P4Hs), also named α2β2 tetrameric α-ketoglutarate-dependent dioxygenase, consists of two α subunits and two β subunits. This isoenzyme hydroxylates proline residues and catalyzes 4-hydroxylation of proline, thus producing collagen triple

helix formations (Jaakkola et al., 2001). This hydroxylation is done in the -Xaa-Pro-Gly- proline sequence (Aro et al., 2012). Hydroxylation of a proline residue in collagen also increases the thermal stability of the triple helix domain (Shoulders & Raines, 2009).

The P4Hs are a group consisting of three isoenzymes C-P4H1, C-P4H2 and C-P4H3 (Rappu et al., 2019) (Figure 3). The α subunit of P4Hs (P4HA) conducts the binding and catalytic activity of the peptides. The β subunit transists α subunit from insoluble to soluble form (Myllyharju & Kivirikko, 2004). P4Hs are necessary because they hydroxylase four proline residues and conduct the accurate folding of collagen polypeptide chains. This folding is essential for triple helical stability (Myllyharju & Kivirikko, 2004).

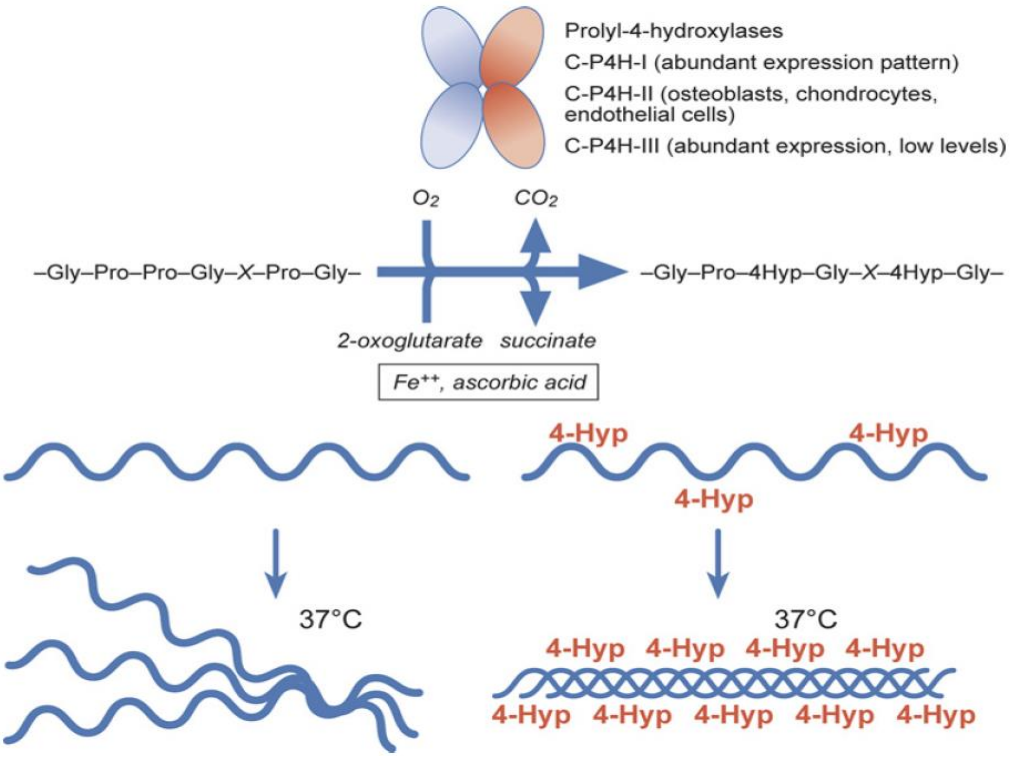

Figure 3. Three isozymes of collagen prolyl 4-hydroxylases (C-P4H1, C-P4H2 and C-P4H3). Hydroxylation of proline residues in collagens both co- and post- translationally requires O_2, 2-oxoglutarate, Fe++, and ascorbic acid. Picture from Rappu *et al*., 2019.

In mammalian cells, three isoforms of P4Hs alpha subunit (P4HA) have been recognized with different α chains. P4HA1 (previously known as P4H1), which is the most abundant

isoform, is found in most cells and tissues where it conducts the major prolyl hydroxylase activities (Annunen *et al*., 1998). This isoform's high expression level leads to profound collagen deposition in cancer development and progression (Li *et al*., 2022). Collagen deposition by P4HA1 is responsible for cancer metastasis and poor cancer prognosis. However, the molecular mechanism of P4HA regulation is still not fully understood. P4HA1 responses to hypoxia and glycolysis in cancer progression. It is crucial in regulating the hypoxia-inducible factor HIF-1 (Xiong *et al*., 2018). Collagen P4H binds to oxygen more efficiently than HIF1-P4Hs. As a result, collagen P4Hs can also function in low oxygen levels. Although collagen deposition is essential for cell and organ differentiation, abnormal PTMs of collagen lead to ECM remodeling, cancer metastasis (Gilkes *et al*., 2013a) and delayed chondrogenesis (Myllyharju & Schipani, 2010). Overexpression of P4HA1 in hypoxia promotes cancer (Zhao & Liu, 2021).

Another isoform of P4HA, P4HA2, also conducts collagen biogenesis and is responsible for ECM remodeling, like P4HA1 (Gilkes *et al*., 2013a). Overexpression of P4HA2 correlates with poor clinical outcome. However, reduced expression was found in breast cancer upon P4HA2 silencing, but still little is known about P4HA2 regulation (Xiong *et al*., 2014). The third isoform, P4HA3, is least known isoform, however, it is responsible for proliferation of cancer cells (Atkinson *et al*., 2019; Eriksson *et al*., 2020).

1.3.2 Collagen lysyl hydroxylase

Collagen lysyl hydroxylase is a major ECM component responsible for collagen biosynthesis. Collagen synthesis by collagen lysyl hydroxylase is a complex process of collagen formation. It plays a crucial role in collagen cross-linking during cancer migration and invasion through extensive post-translational modifications. In addition, collagen cross-linking through hydroxylysine is more stable than cross-linking formed by matrix metalloproteinases (MMPs). Lysyl hydroxylation also works as a carbohydrate attachment site (Gilkes *et al*., 2013b).

Collagen lysyl hydroxylase has at least three isoenzymes (Myllyharju & Kivirikko, 2004), of which PLOD1, PLOD2, and PLOD3 have been identified so far. Different cytokines and transcription factors regulate PLODs expression (Qi & Xu, 2018). One of the critical

factors in cancer, hypoxia, regulates HIF-1, which also modulates PLOD expression. Intratumoral hypoxia is responsible for cancer invasion, and in cancer metastasis PLODs are highly expressed as a consequence of transcriptional regulation (Hofbauer *et al*., 2003; Myllyharju & Schipani, 2010). PLOD1 hydroxylates lysine residues in the triple helix, while PLOD2 hydroxylates lysine residues in telopeptide domains (Yeowell *et al*., 1997). However, PLOD2 is the only lysyl hydroxylase responsible for changes in collagen cross-linking patterns (Wu *et al*., 2006) and promotes fibrosis (Brinckmann *et al*., 1996).

1.4 Laminins, important glycoproteins in the basal membrane

Laminins are a family of conserved, multidomain glycoproteins found in the basement membrane (BM) in all animals (Domogatskaya *et al*., 2012; Rousselle & Scoazec, 2020). They mediate several biological functions, such as cellular interactions, binding with other extracellular matrices, and self-polymerization. Laminins play an essential role in the ECM structure and are involved in the insoluble nature of the ECM.

All laminins consist of three chains, α, β, and γ, assembled into a spiral shape at the C terminal ends. To date, five, four, and three forms of α, β and γ chains are found, respectively (Domogatskaya *et al*., 2012). These heterotrimers together can weigh from 400 to 800 kDa. Fifteen tissue-specific isoforms with distinct functions are identified (Turck *et al*., 2005). Isoforms are named by a combination of the three chains, for example, α4, β1, and γ1 form an isoform named laminin-411 (Domogatskaya *et al*., 2012).

Prior binding to cellular receptors, laminins are modified through proteolytic processing at the N- and C-terminals. This process also alters the signaling pathways in the ECM. For example, laminin-332 binds to α6β4 integrin and develops squamous cell carcinoma (SCC) tumorigenesis through the PI3K activation *in vivo* (Marinkovich, 2007). Laminins also bind to non-integrin receptors, such as dystroglycan, sulfated glycolipids, and 37/67LR which mediate intestinal epithelial cell function and are suggested to be involved in pathological states (Cloutier *et al*., 2019; Mohan *et al*., 1990). However, laminins are also involved in co-signaling with growth factors, making their mechanism and function very complex.

1.4.1 Laminin-332

Laminin-332, previously known as laminin 5, is a cell adhesive molecule present in the basement membrane. It is a large molecular weight glycoprotein and one of the most significant components in the ECM, produced by keratinocytes (Rousselle & Scoazec, 2020). It is recognized as an invasive marker in epithelial tumor cells (Katayama & Sekiguchi, 2004). Laminin-332 maintains the epithelial-mesenchymal cohesion in tissue to protect from external forces on the skin (Brassart-Pasco *et al*., 2020). This protein also plays a crucial role in normal cells, for example in cell differentiation, tissue development, cell adhesion, and wound healing (Kirtonia *et al*., 2022). Laminin-332 is unique from other laminins, as this is the only laminin that contains γ2 chain, and widely spread among epithelia. It is expressed in many pathological states, like in several epithelial cancers, e.g. cutaneous squamous cell carcinoma and oral, cervical, and colon cancers (Calaluce *et al*., 2001; Kirtonia *et al*., 2022; Lohi *et al*., 2000; Siljamäki *et al*., 2020). In different epithelial cancers, laminin-332 is a major component in the BM barrier, and highly relevant for epithelial carcinoma invasion (Guess & Quaranta, 2009).

Laminin-332 is named by its heterotrimeric assembly of α3, β3, and γ2 chains, which forms its cross-checked coiled-coil shape (Katayama & Sekiguchi, 2004). First, disulfide-linked β3-γ2 dimers are formed, followed by α3 alignment, and finally, spiral structure, which takes place in the endoplasmic reticulum. Lastly, α3 and γ2 go through the maturation stage and get into a more diminutive form.

1.4.2 Laminin-332 in cancer

The α3 chain of laminin-332 plays a vital role in cancer progression. Its large globular domain (LG 4,5) cleaved from ordinary skin cells stimulates signaling pathways, influencing tumor growth and migration (Rousselle & Scoazec, 2020). The α3 chain is also involved in tumor growth in nude mice (Mizushima *et al*., 2002). Furthermore, the β3 chain is involved in cancer migration. In 90% of prostate cancer cases, the cleavage of β3 by hepsin protease increases cancer migration (Tripathi *et al*., 2008). On the other hand, the most studied γ2 chain is different from α3 and β3 chains. Unlike α3 and β3 chains, γ2 is produced as a monomer (Gagnoux-Palacios *et al*., 2001). This chain is vital

to laminin-332 incorporation into the basement membrane and regulates adhesive structures called hemidesmosomes. In a monomeric form, it also works as a migratory substrate (Guess & Quaranta, 2009). However, this cleavage of γ2 does not always influence migration (Yurchenco, 2011).

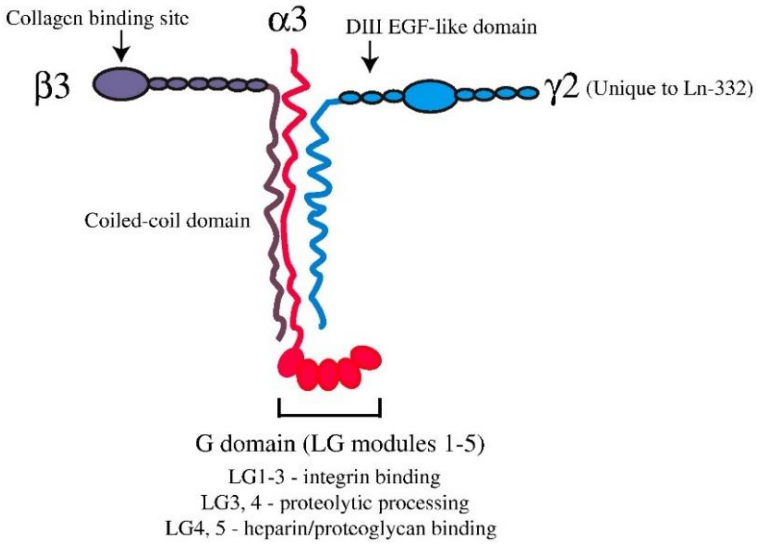

Figure 4. Structure of laminin-332 with binding domains. Heterotrimeric structure consists of long arm coiled-coil feature with integrin and proteoglycan binding domain. Laminin-332 consists of three subunits, α3, β3, and γ2. The short arms β and γ consist of cleavable interaction domains for ECM interaction and signaling functions. Picture from Guess *et al*., 2009.

Proteolytic processing of β3 and γ2 chains is related to cancer invasion and migration in epithelial carcinomas, especially in SCC (Guess & Quaranta, 2009). However, different enzymes, for example enzymes of the astacin family of the MMPs, process α3 and γ2 chains of laminin-332 (Marinkovich, 2007). Laminin-332 interaction with fibrous collagen VII increases collagen type IV and XVIII degradation and peptide production. This process also increases cell invasion. Laminin production correlates with cancer metastasis and poor survival. In addition, laminin-332, especially laminin γ2 chain, is considered as an invasive cancer cell marker (Siljamäki *et al*., 2020; Yamamoto *et al*., 2001). Laminin-332 has been shown to induce PI3K and mitogen-activated protein signaling (MAPK) pathways (Rousselle & Scoazec, 2020). Recently, in cutaneous squamous cell carcinoma, laminin-332 synthesis was shown to be upregulated by

hyperactive H-Ras signaling and fibroblast-activated TGF-β signaling pathways, leading to increased cancer cell invasion (Siljamäki *et al*., 2020).

1.5 Cutaneous squamous cell carcinoma

Cutaneous squamous cell carcinoma (cSCC) is the second most common non-melanoma skin cancer. Among non-melanoma skin cancers, cSCC accounts for 75% of all deaths. The prognosis of treated cSCC is good and the survival for 5 years is ≥ 90% (Fania *et al*., 2021; J. Y. S. Kim *et al*., 2018). However, cSCC can be both locally invasive and metastatic, and the survival rate drops dramatically if the cancer metastases. The major risk factors for cSCC are advanced age, exposure to UV light, immunosuppression, smoking, fair skin, and previous skin cancer history (Paradisi *et al*., 2020; Stratigos *et al*., 2020). However, cSCC progression is a multistage process where mutations in genes play important role. Viral infection, epigenetic modifications or microenvironmental changes are the reasons for gene mutations in cutaneous squamous cell carcinomas. Like in other cancers, tumor microenvironment (TME) is important in the carcinogenesis of cSCC. Epigenetic reprogramming, DNA damaging, hypoxia, CAF and angiogenesis activation, and immune cell recruitment all act as tumor promoters (Fania *et al*., 2021).

Surgical excision is the treatment for the invasive form of cSCC cancer patients, although radiotherapy is also used as a primary treatment for patient who are beyond surgical treatment. The cSCC pathogenic studies enable some pharmaceutical targets recognition and immune therapy as a treatment; however, cSCC diagnostics and prognosis draws less attention than the therapies (Fania *et al*., 2021).

Although the molecular basis of cSCC progression is incompletely understood, mutations in NOTCH pathway, p53 pathway and MAPK and PI3K pathways have been found in cutaneous squamous cell carcinoma (Chang & Shain, 2021). Increased amount of laminin-332 was noted in cSCC cells and transformed keratinocytes due to activation of Ras/ERK and TGF-β/Smad2 signaling pathways, leading to enhanced cancer cell invasion (Siljamäki *et al*., 2020). Recent findings suggest that in addition to Ras and TGF-

β/Smad2 signaling pathways, also TGF-β-activated p38 signaling regulates laminin-332 synthesis in transformed keratinocytes and cSCC cells (Siljamäki *et al*., 2022).

1.6 Tumor microenvironment

Solid tumors are composed not only of tumor cells, but they also consist of the ECM, vasculature, stromal cells, and immune cells. All these elements together are defined as tumor microenvironment (TME) or cancer stroma. TME has a large effect on cancer progression. TME components, along with cancer cells, takes part in cancer progression. Self-produced cytokines and chemokines support cancer cell's growth. Cancer cells can activate surrounding stromal cells like fibroblasts and immune cells. Polymorphonuclear leukocytes (PMN), monocytes, and activated stromal cells produce proteases like matrix metalloproteinases (MMPs). These MMPs are also responsible for ECM degradation (Brassart-Pasco *et al*., 2020). As soon as cancer cells and stromal cells are activated, angiogenesis start to progress. All the elements in TME and ECM dynamics play important role in cancer progression (Balkwill *et al*., 2012).

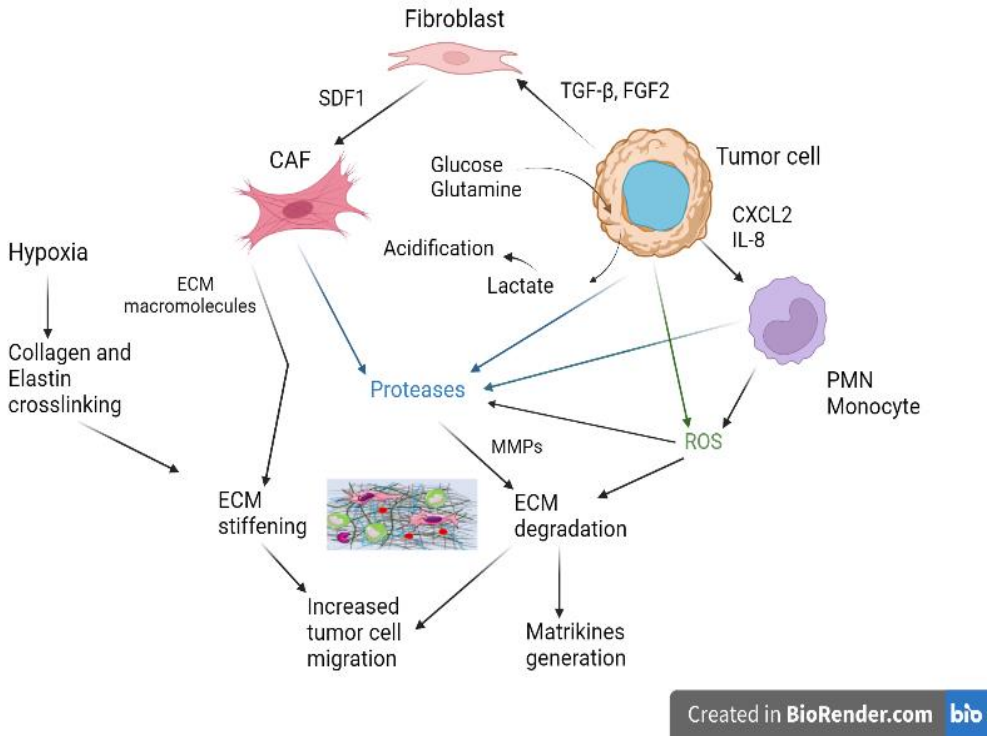

Figure 5. Overall view of the tumor microenvironment (TME) and cancer metastasis. Cancer cells influence nearby stromal cells like fibroblasts. The activated cancer associated fibroblasts (CAFs)

produce proteases like MMPs. CAFs are responsible for ECM stiffening. Degradation of ECM by proteases and ECM stiffening by elastin cross linkage led to cancer progression and metastasis. Growth factors and immune cells secreted by cancer cells take part in cancer cell proliferation. Other effects like hypoxia also influences cancer progression by ECM remodeling. ECM, extracellular matrix; ROS, reactive oxygen species; MMPs, matrix metalloproteinases; SDF1, stromal derived factor 1; CAF, cancer associated fibroblast; IL8, interleukin 8; FGF2, fibroblast growth factor 2, TGF-β, transforming growth factor-β. Image was created in Biorender.com and modified from Brassart-Pasco *et al*., 2020.

1.6.1 Fibroblast

The most abundant stromal cells in the TME are fibroblasts (Brassart-Pasco *et al*., 2020). These cells are flat, spindle-shaped cells with nucleoli. The function of these cells is to produce collagen, proteoglycan, and elastic fiber in normal tissue homeostasis. In addition, fibroblasts are also responsible for supporting ligaments, bone, skin, basement membranes and blood vessels (Kusindarta & Wihadmadyatami, 2018). In embryonic development stage, fibroblasts are significantly activated and exclusively produce matrices tissue. However, they are also found in adult tissue during inflammation and in the tumorigenic environment (LeBleu & Kalluri, 2018).

Fibroblasts play an essential role in cancer progression and immunity (Barrett & Puré, 2020). They influence tumor growth, invasion, angiogenesis, and chemoresistance. They are responsible for growth factors production, thus supporting cell proliferation, migration, and remodeling of the ECM (Attieh *et al*., 2017; Kalluri, 2016).

1.6.2 Cancer-associated fibroblasts (CAFs)

Activated fibroblasts in cancer are called cancer-associated fibroblasts (CAFs). CAFs are also called reactive stromal fibroblasts or tumor-associated fibroblasts. During tumorigenesis, CAFs are activated by different external factors, such as hypoxia, chemokines, cytokines, and TGF-β growth factor (Belhabib *et al*., 2021).

CAFs, together with immune and cancer cells, participate in ECM production, changes, immune reprogramming in TME, and tumor growth. They also modify matrix metalloproteinase production. CAFs have substantial effects on tumor growth and cancer progression. ECM deposition and stiffness promote cancer cell migration, and this modification, in turn, recruits more fibroblasts and help to activate these new fibroblasts. As a result, this initiates more ECM production and progresses cancer metastasis (Belhabib *et al*., 2021; Kalluri, 2016). Due to its importance in cancer progression, CAFs are considered as a therapeutic target in malignant cell targeted therapies (Barrett & Puré, 2020).

1.7 Hypoxia in cancer

Cells are subjected to a wide range of stresses that impact cellular function. Hypoxia is a common stress factor in solid tumors and in TME. Emerging data has confirmed that hypoxia is highly correlated with cell proliferation, differentiation, angiogenesis, genetic modification and instability, tumor invasion, and metastasis (Gilkes *et al*., 2014; King *et al*., 2021; Muz *et al*., 2015). Hypoxia develops in a solid tumor when rapid cell growth resists the oxygen supply in the tumor's inner space. In typical cell environments, oxygen tension is 5-10%, whereas, in hypoxic conditions, it is 1-2% or even lower. The exclusive number of proliferating cells disrupts the regular blood supply in developing cancer tumors. In accordance with hypoxia, angiogenesis causes uncontrolled oxygen supply to these exclusively proliferating cells in the tumor, by forming abnormal blood vessels and impaired blood flow. Furthermore, tumor cells sustain restricted oxygen levels and adapt to survival (Emami Nejad *et al*., 2021; Muz *et al*., 2015; Vinaiphat *et al*., 2021).

In addition, hypoxia is an important factor for cancer cell metabolism and therapy resistance. The hypoxic tumor microenvironment manifests different gene expressions and complex cell signaling stimulation. This signaling cascade results in both positive and negative feedback on cancer (Muz *et al*., 2015). However, hypoxia significantly influences cancer invasion and metastasis and increases tumor survival. In hypoxia, HIF-1α signaling is highly upregulated in different cancers and skeletal dysplasia (Gilkes *et al*., 2013a; Stegen *et al*., 2019). In hypoxic conditions, cancer cells undergo several adaptation processes which are positively correlated with cancer progression and

metastasis. Acute hypoxia induces genetic, molecular, cellular, and biochemical alterations (Emami Nejad *et al*., 2021; Riffle & Hegde, 2017). Moreover, ECM remodeling due to hypoxia is the reason for chemo and drug resistance. Increasing cell mass in the hypoxic region causes chemoresistance by affecting drug delivery (Muz *et al*., 2015). It is also reported that, in hypoxic tumors, cells are more like stem cells, more invasive but less mature (H. Kim *et al*., 2018).

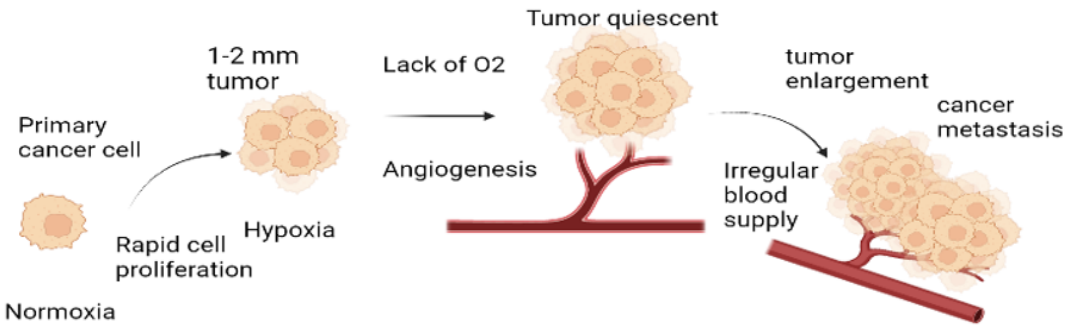

Figure 6. Mechanism of hypoxia-induced tumor progression. Cellular proliferation results in tumor formation. Inner part of the growing tumor lacks oxygen and nutrients due to inaccessible blood vessels. This part is called the hypoxic region. As a result, growth arrest and cell waste accumulate in this region. Tumor cell's alteration in cellular metabolism initiates angiogenesis, and vasculogenesis lead to abnormal blood circulation and cancer growth, and metastasis. Image was created in Biorender.com and modified from Vinaiphat *et al*., 2021.

1.8 ECM remodeling during hypoxia

ECM remodeling is a complex cell regulatory process triggered by different factors, for example, cell stress, heat shock, and hypoxia. Intratumoral hypoxia stimulates ECM production and configuration changes in ECM. Hypoxia-inducible factors (HIFs) are the fundamental regulatory factors for ECM remodeling in hypoxia (Gilkes *et al*., 2013a). This family of transcription factors contains three members, HIF-1, HIF-2, and HIF-3. Among them, HIF-1 is the most studied transcription factor responsible for several gene expressions during hypoxia (Ziello *et al*., 2007). This transcription factor consists of an

oxygen-sensitive HIF-1α containing two proline residues. In normoxia condition, these proline residues are hydroxylated by prolyl hydroxylase domain-containing proteins (PHDs), which results in Von Hippel-Lindau tumor suppressor (pVHL) binding to HIF-1α. HIF-1α binding with pVHL leads to ubiquitination and degradation by 26S proteosome. However, in hypoxia HIF-1α is stabilized and free HIF-1α binds to HIF-1β. This heterodimer then binds to hypoxic response elements (HRE) and express different genes, including vascular endothelial growth factor (VEGF), glucose transporter-1 (GLUT-1) and erythropoietin (Déry *et al*., 2005; Lin *et al*., 2014; Petrova *et al*., 2018). In addition, HIF-1 also activates prolyl hydroxylases (P4HAs) and collagen lysyl hydroxylase (PLOD). P4HAs are responsible for collagen deposition and lysyl hydroxylase is responsible for collagen stiffening, thus collagen fiber alignment. Also another gene, lysyl oxidase (LOX), which is directly regulated by HIF-1α, is highly expressed in hypoxia. Lysyl oxidase family is also responsible for crosslinking of collagen and elastin. Crosslinking, collagen stiffening and fiber alignment enable cancer cell migration and finally cancer metastasis (Gilkes *et al*., 2013a; Xiao & Ge, 2012).

Different cellular processes are involved in the ECM remodeling process, such as angiogenesis, stem cell regulation, and bone remodeling (Karampoga *et al*., 2022). All these cell regulatory processes comprise over 700 proteins. Chemical modifications alter proteins' biochemical properties and structure in the post-translational level. Proteolytic degradation is responsible for migration and invasion by releasing ECM fragments. All the ECM alterations affect complex cellular signaling networks, as ECM components work as ligands for cell surface receptors like integrin and receptor tyrosine kinase. Cancer cells and stromal cells like fibroblasts alter ECM remodeling system to support their own growth. Tumor cells primarily work for recruitment and activation of stromal cells like fibroblasts, and these stromal cells then deposit ECM components in TME by secreting different growth factors, such as TGF-β, FGF, platelet-derived growth factor (PDGF) and epidermal growth factor (EGF). EGF and SDF1 are responsible for activating CAFs, which produce high amount of collagen. Moreover, ECM alteration is prominent in aged tissue. In aged tissue, changes in MMPs and chemokines expression support tumor development (Gilkes *et al*., 2014; Henke *et al*., 2020).

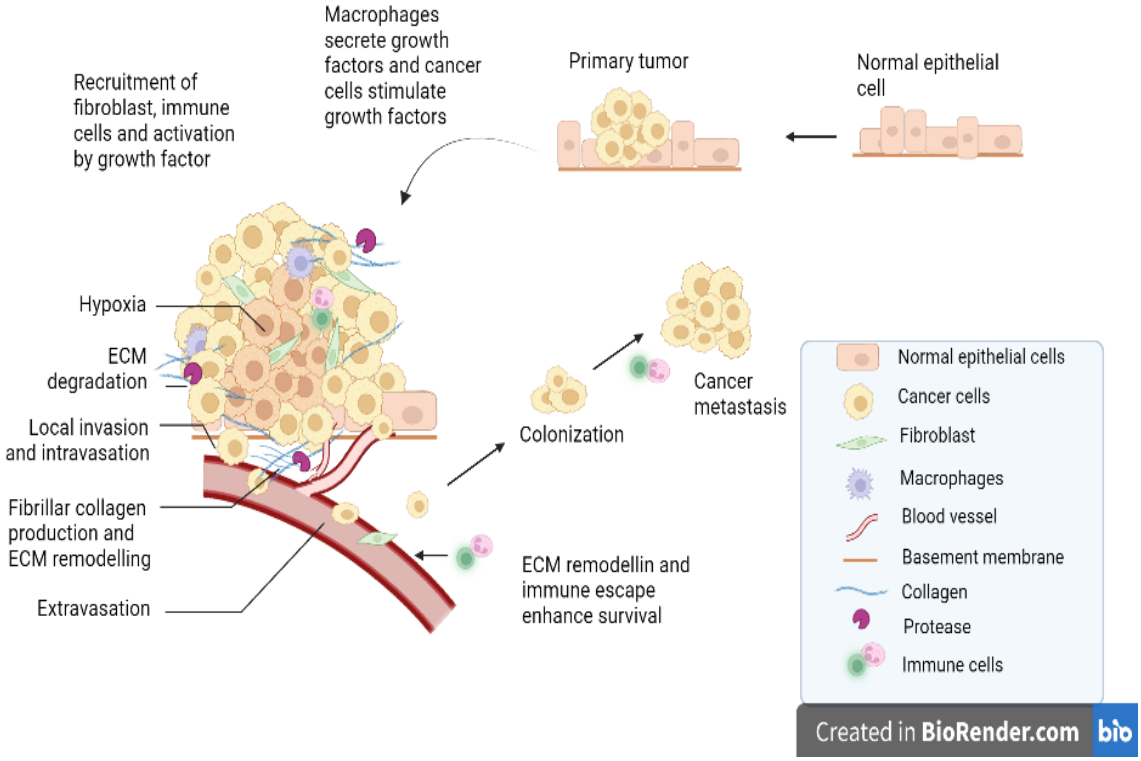

Figure 7. Extracellular matrix remodeling during hypoxia. ECM remodeling is maintained by tissue integrity. Growth factors activated fibroblasts and cancer cells are transcriptionally reprogrammed to produce proteases like MMPs and degrade BM. Proteases also degrade collagen and stiffen collagen fibers, making space for local invasion, intravasation, and cancer metastasis. ECM remodeling and immune cell escape also enhance cancer cell survival. Growth factors retained in tumor microenvironment function as chemotactic signals and recruit and activate more stromal cells, leading to cancer progression. Image was created in Biorender.com and modified from Gilkes *et al.,* 2014 and Boedtkjer *et al*., 2020.

1.9 3D cancer spheroids

Spheroids are highly spherical, multicellular collections, the most common form of three-dimensional cell culture methods (Peirsman *et al*., 2021). In traditional 2D monolayer cell cultures, the cells cannot form the same natural organization as the cells *in vivo* in a tissue. 3D spheroids provide a more tissue-like environment, which enables the cellular interactions that are indispensable for the natural function of the cells. 3D spheroid models are increasingly used in cancer diagnostics and drug treatment as they give more predictive data and relevant information for *in vivo* tests. The 3D cancer spheroids *in vitro*

are more precisely resampled with tumor microenvironment and immune manifestation (Bhattacharya *et al*., 2020). Furthermore, this model defines the complex nature and heterogeneity of cancer tumors *in vivo* and acts as a representative form of therapeutic strategies (Riffle & Hegde, 2017).

The traditional 2D cell culture methods are used in different cell-based assays, although these methods are inefficient in diagnosis and treatment. Drugs tested in traditional 2D cell culture methods are often rejected in drug phage trials: only 10 percent of the drugs are finally approved in the phase III trials (Riffle & Hegde, 2017). Conversely, the 3D spheroid method has been proven to be an efficient method in drug testing, for example, by showing more resistance to anti-cancer drugs (Riffle & Hegde, 2017).

The 3D cell culture method functions differently and exhibits the complex nature of TME compared to the 2D cell culture method; as a result, protein expression also differs in 3D spheroids culture compared to the 2D cell culture method. For instance, many cellular events like cell proliferation, growth, migration, and invasion are different in 3D cell cultures. One of the reasons is that the 3D cell culture method enables efficient cell-to-cell interactions, in addition to cell-to-ECM and cell-to-media interactions (Figure 8). This method also enables the culture of different cell lines, for example, stromal cells with cancer cells together, providing an opportunity to produce a more complex tumor microenvironment *in vitro* (Kapałczyńska *et al*., 2018; Ojalill *et al*., 2020).

In addition, the 3D spheroid model contains a hypoxic region in the inner part of the spheroids that is impossible to form in the 2D cell culture method, where all cells are exposed to cell culture media. 3D spheroids limit oxygen and nutrition flow into the cells resulting in different populations of proliferating, quiescent and necrotic cells. To date, several different 3D culture methods have been developed and adopted for drug discovery, development, and cancer treatment and implemented in the cell-based study for cell-based analysis. Therefore, the 3D spheroid cell culture method is an excellent *in vitro* model to study cell response *in vivo*. However, this system also need optimization. The 3D spheroids model is missing angiogenesis which is obvious in cancer tumorigenesis (Nishida *et al*., 2006).

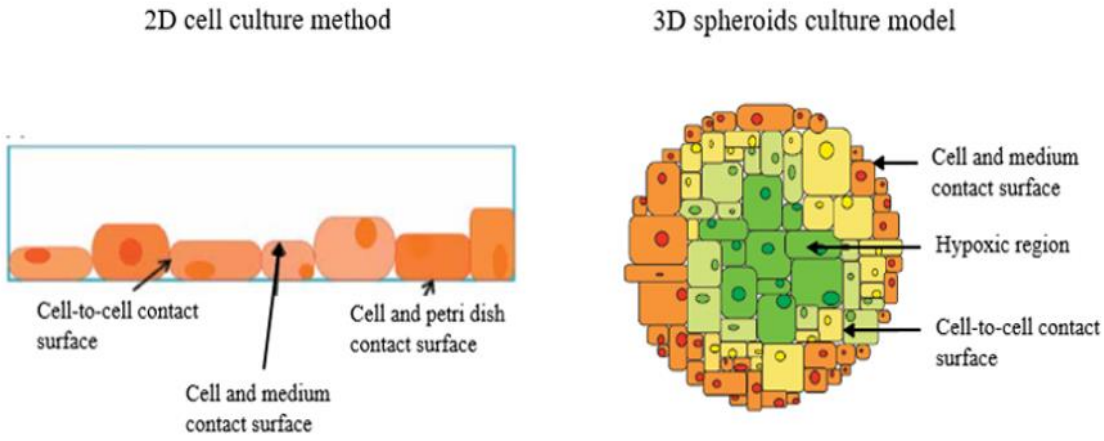

Figure 8. Traditional 2D cell culture and 3D spheroid models. In the 2D cell culture method, cells have more cell-to-media contact and less cell-cell contact. Conversely, in the 3D cell culture model, cells have more contact with the other cells, and only outer cells are in straight contact with the cell culture media. In the 3D spheroids model, different cell zones are observed, such as necrotic core (green), where cells lack oxygen and nutrient; quiescent zone (yellow), where cells already started to grow; and the most outer part (orange) is the proliferative zone. Picture from Kapałczyńska *et al*., 2018.

1.10 Significance of the study

ECM remodeling is a major regulator in cancer progression and metastasis. Hypoxia is one of the main driving factors in this remodeling process. Hypoxia is evident in all cancer tumors and is responsible for drug resistance and poor diagnosis. It modulates cancer cell metabolism and makes a complex signaling network within the TME. Despite the clear evidence that hypoxia has detrimental effects on ECM remodeling and tumor progression and metastasis, no confirmed methods or inhibitors have been discovered to inhibit and treat cancer in hypoxia. The complex nature of ECM modification and signaling cascades during hypoxia within the TME needs further investigation and characterization.

Searching for new drugs for cancer treatment, understanding the mechanism of cancer progression, and early phage diagnosis *in vitro* to apply the drug to patients is a required field to concentrate now. In this study, a new approach to cancer research, the 3D spheroid model, was used, as the nature of 3D spheroids resemble better natural cancer tumors than traditional 2D cell cultures. In addition, laboratory analysis methods such as mass spectrometry, immunofluorescence assay, and western blotting were applied to determine ECM protein regulation and characterize changes in signaling pathways during hypoxia. This study was designed to optimize and characterize a new method for e.g. drug delivery tests in the future. This study provides valuable information about the potentiality of this method when detecting ECM proteins in cancer hypoxia, and it could be a starting point for possible future method development.

2. AIMS OF THE STUDY

The aims of the study were,

2.1 Detection of the ECM proteins in hypoxia: Collagen prolyl hydroxylases (P4HA1 and P4HA2) are crucial for collagen deposition in intratumoral hypoxia and lysyl hydroxylase (PLOD2) is responsible for stiffness in the ECM. The aim was to observe the expression of these proteins in cancer cells during normoxia (21% O_2) and in hypoxia (3% O_2). Elevated expression of the glycoprotein laminin-332 is also prominent feature in cancers, e.g. in cutaneous squamous cell carcinoma. Therefore, we also tested if laminin-332 expression was modulated in hypoxic conditions.

2.2. Demonstrating a new method to detect protein changes in hypoxic conditions. For this reason, a comparatively new model, cancer 3D spheroid model, was used to observe different protein (especially P4HA1, P4HA2, PLOD2, and laminin-332) levels in normoxia and hypoxia. The 3D spheroid method allowed us to coculture cancer cells with stromal fibroblasts, which are known regulators of cancer cell behavior and signaling pathways. In addition, western blot, immunofluorescence, and mass spectrometry were performed to evaluate the protein expression changes in the ECM during hypoxia.

3. MATERIALS AND METHODS

3.1 Cell lines

The H-Ras-transformed tumorigenic HaCaT cell line RT3 (Boukamp *et al*., 1990) and the cutaneous squamous carcinoma cell line (UT-SCC-7) were used as cancer cell lines. The RT3 cell line was provided by Dr. Norbert Fusenig (German Cancer Research Center, Heidelberg, Germany). This cell line is immortalized non-tumorigenic human keratinocyte cell line and one of the HaCaT's retrovirally H-Ras transformed subclones which becomes metastatic after subcutaneous injection into athymic nude mice (Siljamäki *et al*., 2020). The UT-SCC-7 cell line was established from surgically removed metastatic UT-SCC-7 of the skin from a patient of Turku University Hospital (Junttila *et al*., 2007), and is a kind gift from professor Veli-Matti Kähäri (Department of Dermatology, University of Turku and Turku University Hospital, Turku, Finland). Professor Risto Penttinen provided primary human adult skin fibroblasts used in this study. The fibroblasts were from the Medical Biochemistry / the University of Turku's cell line biobank and were used up to passage 12. The donor was male aged 24 years.

3.2 Cell culture

3.2.1 Procedure of 2D cell culture

Cells were grown on a 10 cm Petri dish in Dulbecco's Modified Eagle's medium (DMEM with 4.5 g/L glucose; 12-614F, Lonza), supplemented with 10% Fetal calf serum (FCS, Biowest), L-glutamine (6 nmol/L, Gibco), and 1% penicillin-streptomycin. Additional geneticin-418 selective antibiotic (200 μg/ml, Gibco) was added to the medium during the RT3 cell line culture. The culture medium of UT-SCC-7 cell line was supplemented with 1 x MEM non-essential amino acids (11140-035, Gibco). All cell lines were incubated in an incubator at 37°C in a 5% CO_2-humidified atmosphere. The medium was changed every other day until the cells reached 80%-90% confluency.

3.2.2 3D spheroid formation

The current study used the micro mold method for 3D spheroid formation. Molds consisting of 35 wells were prepared with 2% agarose mixed in 0.9% NaCl using commercial molds (MicroTissues 3D Petri Dish micro mold, Z764051, Sigma-Aldrich). Only cancer cells were used in monocultures, but in cocultures, cancer cells and skin primary fibroblasts were used in a 1:1 ratio. Each spheroid contained 7,000 and 14,000 cells in monoculture and coculture, respectively. The cell culture plates were washed with phosphate-buffered saline (PBS, 17-516 F, Lonza), and the cells were detached from the culture dish with Trypsin-EDTA (ethylenediaminetetraacetic acid, Lonza). Trypsin inhibitor (T9128, Sigma Aldrich) was used at 1 mg/ml into the plate to inhibit trypsin action, followed by centrifugation at 1370 rpm for 4 min at room temperature (RT). Cells were suspended in serum-free DMEM medium supplemented with L-glutamine (6 nmol/L) and 1% penicillin-streptomycin and counted in a cell counter (BIO-RAD, TC10).

The correct number of cells was suspended in serum-free DMEM medium and pipetted into a 50ml falcon tube. In each mold, 80µl of cells suspended in serum-free DMEM medium was pipetted into an agarose mold, followed by a 15 min incubation at 37°C in 5% CO_2-humidified incubator. Next, 1 ml of serum-free DMEM was added surrounding the mold. Ascorbic acid (50 µg/ml; A4544-25G, Sigma-Aldrich) was added daily.

3D spheroids were allowed to grow in an incubator in normoxia (21% O_2) or hypoxia (3% O_2) at 37°C in 5% CO_2 until day 6 (Figure 9). Spheroid samples were collected three times: day 1, day 4, and day 6. The 3D spheroids were imaged with the EVOS cell imaging system (EVOS M500, Invitrogen) using a 4x objective.

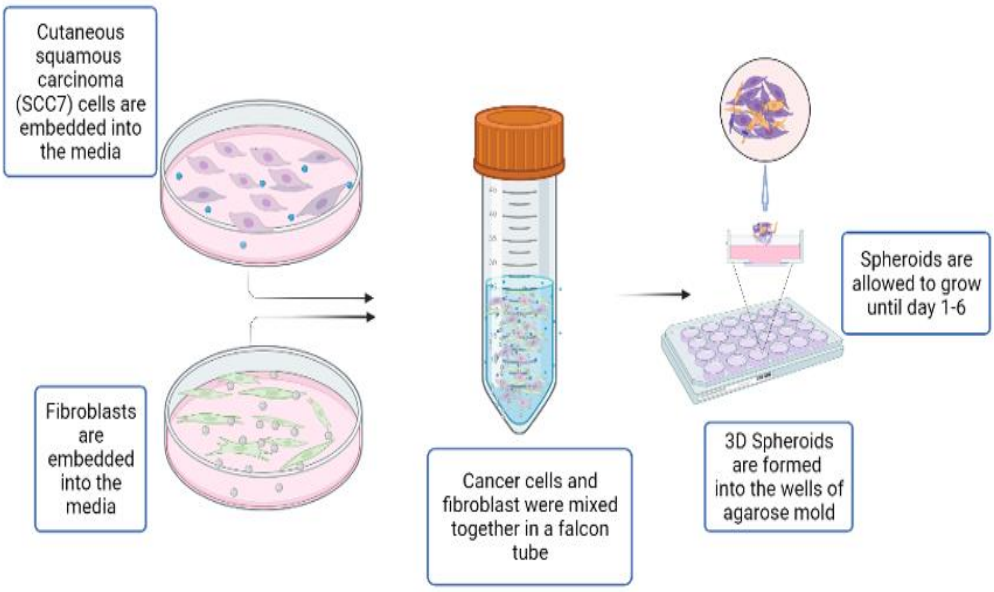

Figure 9. Flow chart of 3D spheroid formation from 2D cell culture. Cancer cells were detached, calculated, mixed with fibroblasts in a falcon tube, and put into the agarose mold. Spheroids were allowed to grow until day 6. Three replicates (i.e., three molds) were made both for normoxia and hypoxia samples. Image was created on Biorender.com.

3.3 Western blot

Western blot is a widely used analytical technique to identify specific proteins in a heterogeneous mixture. In this method, proteins were separated by SDS-PAGE (sodium dodecyl sulfate-polyacrylamide gel electrophoresis) based on their molecular weight and transferred to a nitrocellulose membrane followed by incubation with specific primary and secondary antibodies specific to the protein of interest. Finally, the image was visualized by a luminescent image analyzer. β-tubulin was used as a loading control. The data were normalized against loading control. Finally, images were quantified with ImageJ software.

3.3.1 Sample preparation for western blot

3D spheroids were washed with PBS and collected in an Eppendorf tube for western blot analysis. They were centrifuged at 12000 x g for 4 min, and the pellets were lyzed with radioimmunoprecipitation assay buffer (RIPA Lysis and Extraction Buffer, 89900, Thermo Fisher Scientific). The amount of RIPA buffer was adjusted according to pellet size from 50 µl to 100 µl. Finally, the lysate was preserved at -20^0C. 3D spheroids stored in RIPA buffer were thawed on ice for western blot running. SDS buffer (30% [w/v] glycerol; 10% [w/v] sodium dodecyl sulfate); 9.3% [w/v] DTT; bromophenol blue; 0.35 M Tris-HCl pH 6.8) was added to the sample according to the RIPA buffer amount (sample and SDS ratio 6:1). A sample mixed with SDS was then incubated in the water bath at 100ºC for 10 min and centrifuged at 11000 x g for 1 min.

3.3.2 Sample run

From each sample, 25µl was loaded in one well of 8% or 10% SDS-PAGE (upper gel: 4% [w / v] acrylamide bisacrylamide [35.5: 1, BIO-RAD]; 0.1 M Tris-HCl pH 6.8; 0.05% [w / v] ammonium persulfate (APS); 0.2% [w / v] tetramethylethylenediamine [TEMED]; bottom gel: 8% or 10% [w / v] acrylamide bisacrylamide; 0.4 M Tris-HCl pH 8.8; 0.033% [w / v] APS; 0.067% [w / v] TEMED) gel. A molecular weight standard (Bluestar Prestained Protein Marker Plus, Nippon Genetics) was added to determine the size of the protein. Samples were run in running buffer (25 mM Tris hydroxymethyl aminomethane (Tris); 12.5 mM glycine; 3.5 mM SDS) for 30 min at 70V. After that, the voltage was changed to 130V and run for 90 min. After gel electrophoresis, the gel was transferred to the nitrocellulose membrane (Nitro Bind, Cast, Pure Nitrocellulose, ** Micron, GVS North America) on 350mA at 4 ºC for 100min in transfer buffer (25 mM Tris hydroxymethyl aminomethane [Tris]); 12.5 mM glycine; 20% [v/v] methanol).

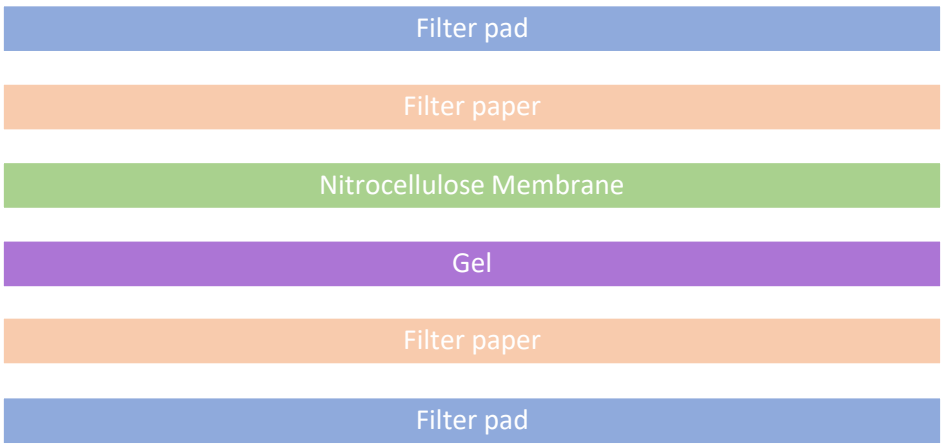

Figure 10: The orientation of a gel sandwich used for protein transfer on nitrocellulose membrane. Nitrocellulose membrane and gel were placed between transfer buffer-soaked filter papers. Fiber pads were placed at each end of the sandwich.

3.3.3 Blocking, antibody incubation, and detection of protein

After protein transfer, the nitrocellulose membrane was blocked with blocking buffer (5% [w/v] milk-tris buffered saline with Tween [TBST]) for 60 min under shaking at room RT. Then the membrane was washed 3 x 15 min with TBST and incubated with primary antibodies (Table 1) diluted in 1:1000-2000 in 5% [w/v] BSA-TBST overnight at 4°C. The next day, the membrane was washed with TBST 3 x 10 min and incubated with a secondary antibody (Table 1) diluted in 1:8000 in 5% [w/v] BSA (bovine serum albumin)-TBST. The secondary antibody was incubated for 1 hour at RT and protected from light. Next, the membrane was washed as before, and scanning was performed with an Odyssey membrane scanner (Odyssey CLX, LI-COR). β-tubulin was used as a loading control, diluted in 1:16000 in 5% [w/v] BSA-TBST with overnight incubation at 4°C. Then the membrane was washed and incubated with the secondary antibody described before. ImageJ studio software (LI-COR) was used to analyze western blot data. Average from three independent biological replicates was calculated. For analysis, all proteins were normalized against β-tubulin.

Table 1: All primary and secondary antibodies used in western blot.

Primary antibody	**Catalog number**	**Supplier**
P4HA1	ab 244302	Abcam, UK
P4HA2	ab 70887	Abcam, UK
PLOD2	ab 90088	Abcam, UK
Lam-332	ab 14509	Abcam, UK
p-Smad2	3108	Cell Signaling Technology, USA
p-CREB	9198	Cell Signaling Technology, USA
p-ERK1/2	9101	Cell Signaling Technology, USA
β-tubulin	P6154-500GR	BIOTOP
Secondary antibody	**Catalog number**	**Supplier**
Anti-rabbit 800	926-32213	LI-COR, USA
Anti-rabbit 680	926-68071	LI-COR, USA
Anti-mouse 800	926-32212	LI-COR, USA
Anti-mouse 680	926-68072	LI-COR, USA

3.4 Proliferation measurement by Qubit assay

Spheroids prepared in section 3.2.2 were used for DNA isolation and measured by Qubit assay (Q-32851, Invitrogen-Thermo Fisher Scientific, USA). This broadly used method utilizes optimized dyes that bind to DNA and provide sensitive detection. First, DNA isolation was performed according to the manufacturer's instructions (740609.250, Macherey-Nagel GmbH & Co.KG). Then, the Qubit working solution was prepared by diluting the dsDNA HS reagent (Q-32851 A, Invitrogen-Thermo Fisher Scientific) with dsDNA HS buffer in 1:200 dilution. Two standard solutions, 0 ng/µl (Q-32851 C, Invitrogen-Thermo Fisher Scientific, USA) and 10 ng/µl (Q-32851 D, Invitrogen-Thermo Fisher Scientific, USA), were used as a 1:20 ratio in the working solution to calibrate the machine. For the sample measurement, 1 µl sample was added into 199 µl working solution and incubated for 3 min. The DNA amount was multiplied 200 times as the measurement was made from a sample diluted 1:200. Average from three independent biological replicates was calculated.

3.5. Immunofluorescence

Immunofluorescence is a method to detect antibodies with fluorescence dye to visualize antigens under a light microscope. It is used in cultured cells in 2D cell culture and 3D spheroids and single-cell and tissue sections. Immunostaining, using antibodies to stain proteins, is a widely used example of immunofluorescence. Confocal microscopy imaging systems were used to get high-resolution images.

3.5.1 CellTracker staining of cultured cells

2D cancer cell and fibroblast cultures described in 3.2.1 were used for CellTracker staining. Cell culture media was replaced with fresh DMEM supplemented with 10% FCS. CellTracker Orange (C34551, Invitrogen) for cancer cells and green (C7025, Invitrogen) for fibroblasts were used to stain the cells and diluted into 9.1 µl of dimethyl sulfoxide (DMSO). Then the diluted solution was suspended again 1:50 in DMSO. 62,5 µl of the diluted CellTracker was added to each 10 cm cell culture plate containing 5 ml culture medium. Careful shaking was done to confirm even spreading of CellTracker dye. Then cells were incubated for 1 h at 37 °C and washed briefly twice with PBS. 5-10 ml of DMEM supplemented with 10% FCS was added to cells, followed by 15 min incubation at 37 °C. After that, 3D spheroids were formed according to the described method in 3.2.2 and incubated in both normoxia (21% O_2) and hypoxia (3% O_2) incubators. Cells were protected from light in all steps of cell staining.

3.5.2 Spheroid staining with P4HA1 antibody

3D spheroids stained with CellTracker were cultured for 3 days, and the growth medium was discarded. Then spheroids were washed out of the agarose mold with PBS buffer, followed by spheroid fixation with 4% paraformaldehyde (PFA) for 1 h at 4°C. Then, spheroids were incubated for 1.5 hours at 4°C with 4% PFA supplemented with Triton X-100 (1%) for further fixation. After that, spheroids were washed with PBS with 0.1% Tween-20 (PBST), and blocking was performed with 6% BSA-PBST for 3 hours at RT. Next, 3D spheroids were incubated with prolyl 4-hydroxylase subunit alpha-1 antibody

(P4HA1, ab 244302, Abcam, UK), diluted in PBST in 1:100 dilution ratio, overnight at +4°C on a shaker. The following day, spheroids were washed with PBST for 3 x 15 min and incubated with secondary antibody (Alexa Fluor 633 goat anti-rabbit, A21094, Invitrogen), diluted 1:200 in PBST for 3 hours at RT. After that, the spheroids were washed with PBS for 3 x 15 min and mounted on coverslips (25 mm x 75 mm x 1 mm glass slide) with 95-100% glycerol.

3.5.3 Confocal imaging

Confocal microscopy is an optical imaging system for increased image resolution and contrast. It is used for example for three-dimensional structure imaging by capturing multiple two-dimensional images. In the current study, a confocal microscope, Zeiss LSM 880 (Zeiss, Jena, Germany), was used for super-resolution imaging for fixed samples. Imaging was performed at the Cell Imaging and Cytometry Core, Turku Bioscience Centre, Turku, Finland, with the support of Biocenter Finland. A Zeiss Plan-apochromatic 20x/0.8 M27 with 543nm HeNe laser and airy can Multitrack ILEX setup was used to capture the images. Three channels were used separately, 647 channels for secondary antibody excitation (Alexa Fluor-633), 561 channels for orange CellTracker excitation, and 488 channel for green CellTracker excitation. The image size was 1024 x 1024 pixels with a maximum speed of 8, and the actual size of the images was 607.3 µm x 607.3 µm. The pinhole was 71.1, and 12 slides in Z-stacks were used in the setting. The images were processed with Zen 2.3 SPI Black software. Spheroids were located on the slide under the laser and selected on the screen. Spheroids were imaged for both hypoxia and normoxia conditions. The intensity was measured with ImageJ software.

3.5.4 Spheroids intensity profile

3D spheroid intensity was calculated by ImageJ software, and intensity was normalized against the distances from the spheroids edge by lining up spheroid’s diameter. This normalization was done to assess spheroids' intensity relative to distance. The intensity values were taken from the middle z-stack of confocal images for all three channels (RT3, fibroblast, and P4HA1), and spheroids diameter was determined using the plot profile in

ImageJ. All calculation was done for three channels separately. To compare intensity between normoxia and hypoxia, intensity was measured in total area for all three channels. This data was shown as intensity value in percent (%) and normalized against the total area. Three spheroids from each normoxia and hypoxia treatment were analyzed.

3.6. Mass spectrometry sample preparation

3.6.1 Hypotonic degradation

3D spheroids were prepared according to the previously described method (3.2.2) and collected on day 4 from the normoxia and hypoxia incubator. Ascorbic acid added to serum-free media was exchanged once during the time. Spheroids were collected in a 24-well plate in PBS. For each mold, 100 µl of hypotonic lysis buffer (10 mM Tris-HCl, pH 7.5; 1 mM EDTA, 10 µg / ml DNAse) was used. All spheroids from each sample were collected into an Eppendorf tube and centrifuged for 2 min at 3900 rpm, followed by a hypotonic lysis buffer wash. Centrifugation was repeated once, and 150 µl of hypotonic lysis buffer was added to the Eppendorf tube. Samples were incubated overnight at +4 °C on a rotator. The following day, spheroids were washed twice with hypotonic buffer and centrifuged for 2 min at 3900 rpm. Finally, the pellet was collected and preserved at -20 °C for peptide preparation and mass spectrometry analysis.

3.6.2 Filter-aided sample preparation

Spheroids treated with hypotonic lysed buffer were added to a solution containing 5% SDS, 0.1 M DTT (dithiothreitol, Thermo Scientific, USA), and 5 mM TEAB (Triethylammonium bicarbonate, T7408, Sigma Aldrich), and heated at 95 °C for 5 min. Then lysate was centrifuged at 16000 x g for 5 min. Protein concentration for each sample was determined to confirm enough protein in the sample by Pierce 660 assay (22660, Thermo Scientific), according to the manufacturer's instructions. Then lysate up to 100 µl was suspended in UA solution, mixed with 8M Urea (51456-500G, Sigma) and 0.1 M Tris/HCl pH 8.5, and centrifuged at 14000 x g for 40 min. This step was repeated until all lysate was used. Again, 200 µl of UA was pipetted into the filter and centrifuged at

14000 x g for 40 min at 20 °C. Next, 100 µl IAA solution (0.05 M iodoacetamide in UA) was added to the sample and mixed in a shaker at 37°C, and incubated at RT for 30 min.

After that, centrifugation was performed at 14000 x g for 40 min, and the step was repeated twice by adding 100 µl of UA to the filter unit. Then, 100 µl of DB (1M urea in 0.1 M Tris/HCl, pH 8.5) was added, and centrifugation was performed at 14000 x g for 40 min. This step was repeated once. Finally, the filter unit was transferred to a new collection tube, and 40 µl of Lys-C/Trypsin (Promega, 5073) mixed DB was added (enzyme to protein ratio 1:25) and mixed in a shaker at 37 °C. Incubation was done at 37 °C overnight. The following day, 100 µl of 0.1 M Tris/HCl, pH 8.5 was added and centrifuged at 14000 x g for 40 min, repeated the step, and combined the filters.

3.6.3 Desalting of sample

After collecting the peptides, desalting was done by adding 10% to 0.5% trifluoroacetic acid (TFA) until it reached pH 2-3. Microcon 10 kDa, a centrifugal unit with ultracel – 10 membrane tips, was used in the desalting step. Tips were put into an Eppendorf tube with a hole in the lid. Then 200 µl of the sample was used in each batch, and a solution mixed with 0.1% TFA and 2% acetonitrile (ACN) was used until all samples were pipetted. Next, samples were spin for 3-4 min at 1.7 x g. After that, the sample was washed three times with 50 µl of 0.1% TFA and 2% ACN and centrifuged for 60 s at 1.7 x g. For the peptide elution, 50 µl of 0.1% TFA, 2% ACN and 0.1% formic acid were used and pushed to the tips and collected to a new Eppendorf tube. Samples were dried in SpeedVac (Thermo Fisher Scientific, USA) and preserved in -20 °C. Finally, samples were dissolved in 1% formic acid for using liquid chromatography-mass spectrometry analysis.

3.6.4 Liquid Chromatography-Tandem mass spectrometry

In mass spectrometry (MS), the peptide analysis was performed using nanoflow HPLC system (Easy-nLC1000, Thermo Fisher Scientific) coupled with a Q Exactive mass spectrometer (Thermo Fisher Scientific). The peptide mixture was separated using a 15 cm C18 column (75 µm x 15 cm, reproSil-our 3 µm 200 Å c18-AQ, dr. Maisch HPLC GmbH, Ammerbuch-Entringen, Germany) with two solvents gradients (Solvent A, 0.1% formic acid and Solvent B, acetonitrile/water, 95.5 v/v with 0.1% formic acid). A complete mass scan was acquired over m / z, and the process was repeated until the gradient ended.

After data acquisition, Spectroanut proteomics software was used for the data analysis. Tandem mass spectra were searched using human SwissProt entries in the UniprotKB database. The false discovery rate threshold for protein identification was set to 0.001, and at least one replicate run of the sample was considered.

3.7. Statistical data analysis

Three independent biological experiments were performed, and the results are shown as mean ± standard error of the mean (S.E.M) value, also stated in the figure legends. Western blot statistical analyses were performed using IBM SPSS statistics version 27. To assess the statistical significance of western blot data, one-way ANOVA (analysis of variance) test was performed. The significance level was set to 0.05, so only *p* values below 0.05 were considered statistically significant. Independent-samples t-tests were used to calculate the *p*-value. GraphPad Prism-9 software was also used to perform statistical analysis and data visualization format preparation for immunofluorescence data. Technical replicates were considered for calculating *p*-value calculation of immunofluorescence data.

4. RESULTS

4.1 Morphology analysis of 3D spheroids

3D spheroids of cutaneous squamous cancer cells (UT-SCC-7) and H-Ras transformed keratinocytes (RT3) cells were used in this study. 3D spheroids were established using a micro mold method. Both cell lines were used to form monoculture spheroids without fibroblasts (Figure 11A, 12A) and coculture with skin primary fibroblasts (Figure 11B, 12B). The microscope images showed that cells started to spread gradually from day 1 to day 6 in both normoxia and hypoxia conditions and in monoculture and in coculture. Interestingly, more tight spheroids were formed in hypoxia in coculture (Figure 11B, 12B).

The proliferation zone was visible in monoculture for UT-SCC-7 and RT3 spheroids. However, no other zones were adequately detectable. In the cocultured 3D spheroids, all three zones, i.e. the necrotic core, quiescent zone, and proliferating zone, are recognizable in both cell lines (Figure 11B, 12B). The cell amount was measured before preparing a mold in a cell counter to confirm each spheroid contains an equal number of cells.

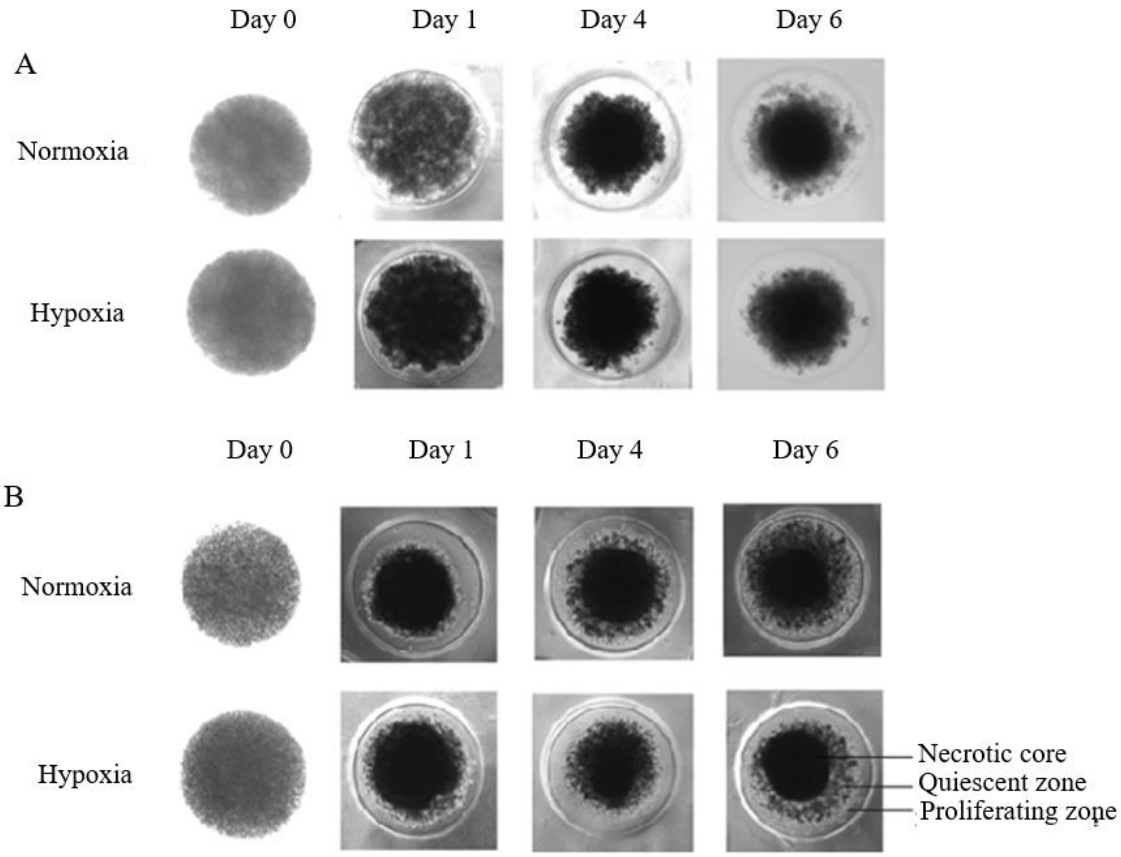

Figure 11. UT-SCC-7 cells in monoculture (A) and coculture (B) with skin primary fibroblasts both in normoxia (21% O_2) and hypoxia (3% O_2). A) Different zones of a typical spheroid are not clearly recognized in UT-SCC-7 monoculture; however, proliferation is visible in each 3D spheroid during culture from day 1 to day 6. B) Coculture of UT-SCC-7 with skin primary fibroblasts resulted in tight spheroids both in normoxia (21% O_2) and hypoxia (3% O_2). Necrotic core, quiescent zone and proliferative zone are visible in day six culture. Spheroids were imaged with the EVOS cell imaging system (EVOS M500) using a 4x objective.

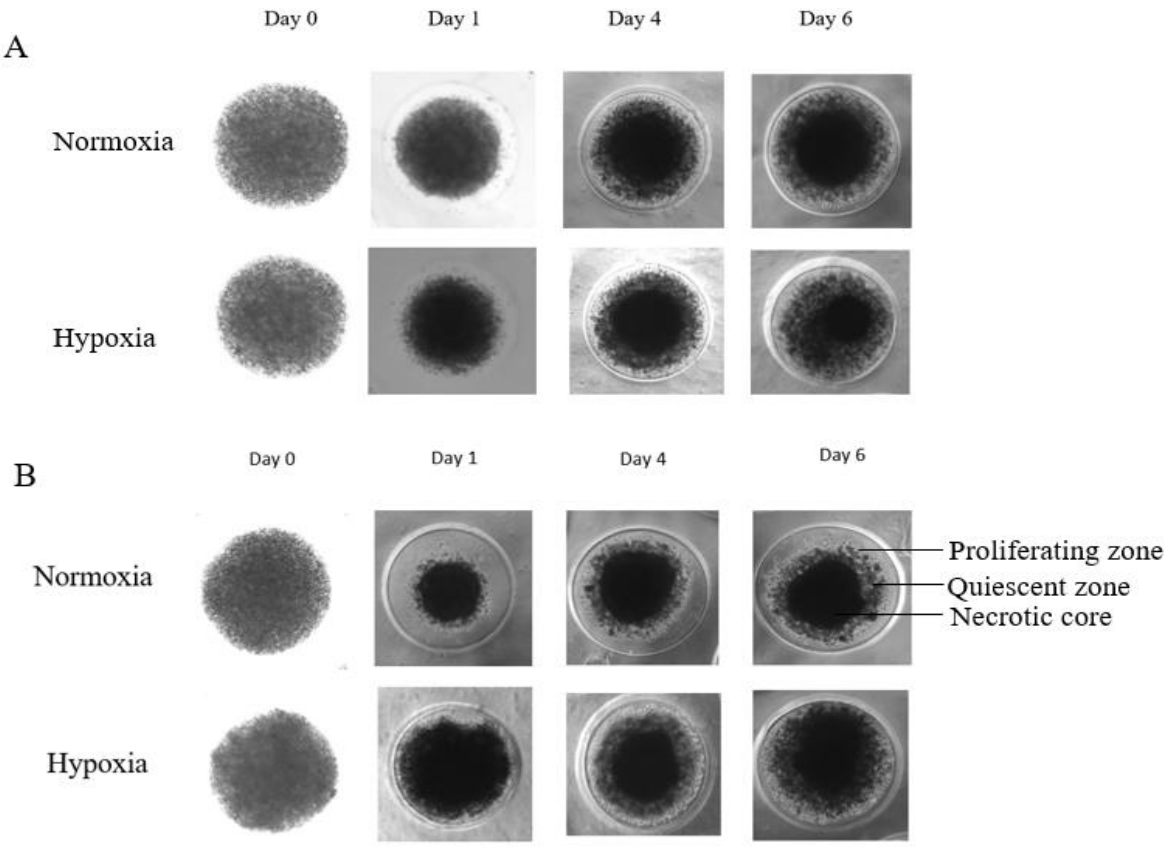

Figure 12. RT3 cells in monoculture (A) and coculture (B) with skin primary fibroblasts in normoxia (21% O_2) and hypoxia (3% O_2). A) Different zones of a typical spheroid are not recognizable in RT3 monoculture, but proliferation is visible in each 3D spheroid during the culture from day 1 to day 6. B) Cocultured RT3 cells with skin primary fibroblasts formed tight 3D spheroids both in normoxia (21% O_2) and hypoxia (3% O_2). The necrotic core, quiescent zone and proliferative zone are visible in day six culture. Spheroids were imaged with the EVOS cell imaging system (EVOS M500) using a 4x objective.

4.2 Hypoxia induced RT3 cell proliferation in 3D spheroids

To investigate RT3 (H-Ras transformed keratinocytes) cell proliferation in normoxia and hypoxia, cultured 3D spheroids were subjected to Qubit assay to assess the DNA amount of the cells. The experiment was performed in monoculture and coculture conditions at four timepoints. The results show that cell proliferation was upregulated, albeit not significantly, in hypoxia compared to normoxia both in monocultures and in cocultures.

However, the cell proliferation rate was reduced after day 4. The proliferation rate at different time points is shown in Figure 13.

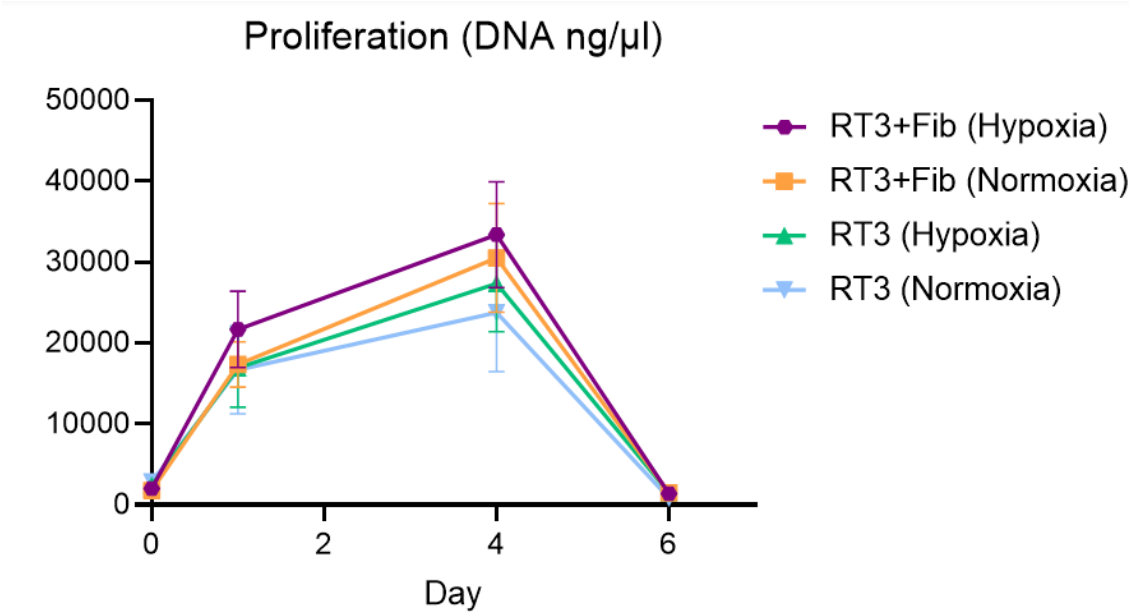

Day	RT3+Fib (Hypoxia)	RT3+Fib (Normoxia)	RT3 (Hypoxia)	RT3 (Normoxia)
0	2006	1765	2400	2836
1	21684	17370	16918	16682
4	33404	30531	27343	23760
6	1409	1493	1469	863

Figure 13. RT3 cell proliferation in monoculture and coculture. DNA amount was determined in normoxia (21 % O_2) and hypoxia (3 % O_2). The graph shows the mean from three independent biological replicates ± S.E.M.

4.3 Hypoxia upregulated collagen prolyl hydroxylases and lysyl hydroxylase expression

Collagen is the most abundant protein in the human body and one of the vital fibrous proteins. It modulates cell behavior and is responsible for ECM remodeling through collagen biogenesis. An increased amount of ECM fiber and collagen stiffness is characterized in cancer (Levental *et al.*, 2009; Provenzano *et al.*, 2009). As hypoxia regulates collagen deposition in the ECM (Gilkes *et al.*, 2013a), we tested whether hypoxic conditions would alter P4HA1, P4HA2, and PLOD2 synthesis in our 3D spheroid

model. UT-SCC-7 and RT3 cells were cultured as spheroids with or without skin primary fibroblasts in normoxic or hypoxic condition. The spheroids were allowed to grow for one to five days before harvesting for western blotting.

In UT-SCC-7 monocultured spheroids, P4HA1 protein level was profoundly upregulated in hypoxia on day 5 compared to normoxia. In normoxia, P4HA1 expression was downregulated gradually until day 5. P4HA2 and PLOD2 proteins were also elevated in hypoxia on day 5. Interestingly, P4HA2 was upregulated in normoxia on day 5, and this trend was similar in hypoxia (Figure 14A, B). However, upregulation of PLOD2 was more notable in hypoxia than normoxia at day 5 (Figure 14B). In cocultured spheroids of UT-SCC-7 cells and skin fibroblasts, the synthesis of all three proteins (P4HA1, P4HA2, and PLOD2) was highly, although not statistically significantly, induced in hypoxia compared to normoxia from day 1 to day 5. The synthesis of these proteins was also increased in normoxia on day 5 (Figure 14C, D); however, the increase was not as prominent as in hypoxia on day 5 (Figure 14C). The average expression of these three proteins from three different replicates showed a notable increase in hypoxia compared to normoxia at day 5 after normalization of proteins expression against β-tubulin (Figure 14D). Previously it has been shown that Hypoxia-inducible Factor 1 (HIF-1) induces P4HA1, P4HA2, and PLOD2 expression in fibroblasts in hypoxic conditions (Gilkes *et al*., 2013a). Our results are in accordance with that finding, as the protein expressions increased when the fibroblasts were present. However, our results were not statistically significant. In addition, our results show that the 3D spheroid model, especially coculture model with fibroblasts, is a promising tool in detecting ECM remodeling in hypoxia.

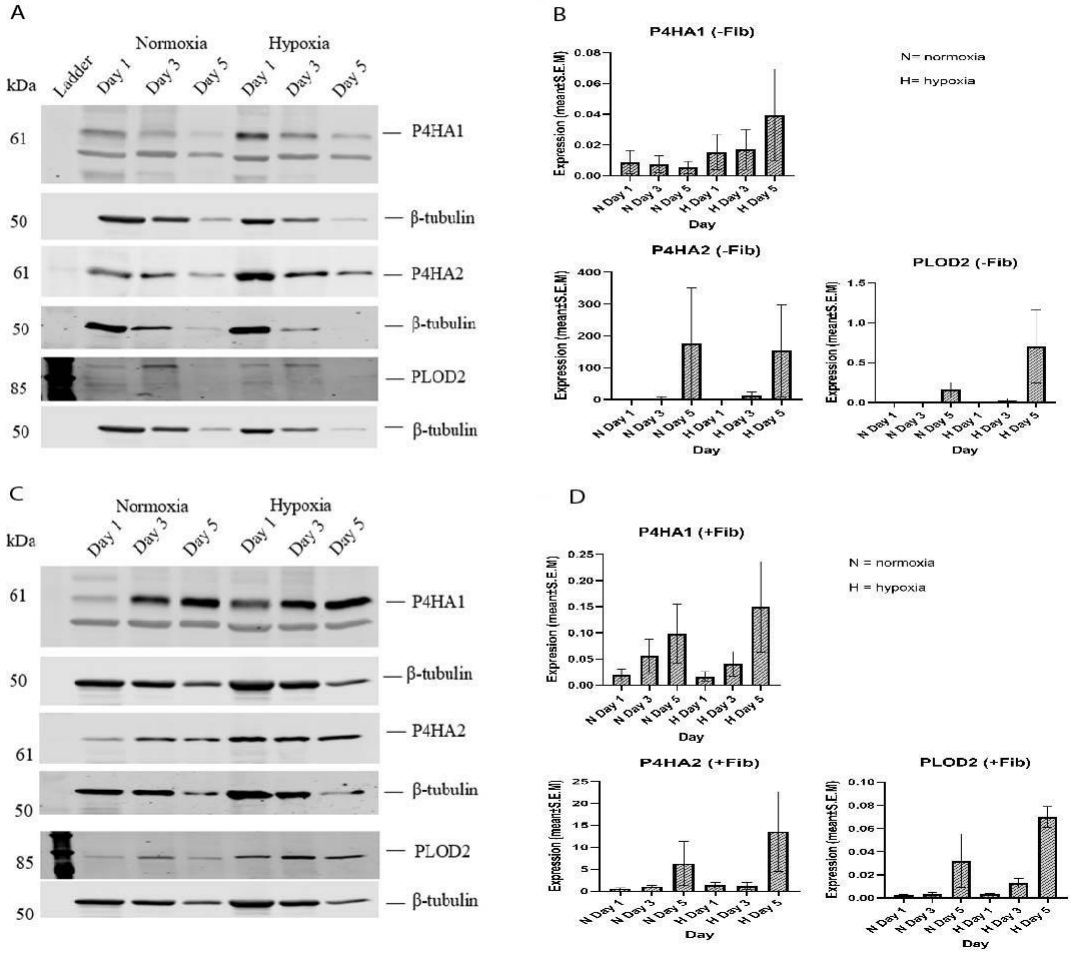

Figure 14. Expression of collagen prolyl hydroxylases (P4HA1 and P4HA2) and collagen lysyl hydroxylase (PLOD2) in UT-SCC-7 cells with and without skin fibroblasts. A) Metastatic UT-SCC-7 cell line was cultured in 3D spheroids in monoculture in both normoxia (21 % O_2) and hypoxia (3 % O_2) for five days, and expressions of P4HA1, P4HA2, and PLOD2 were analyzed by western blot method. β-tubulin was used as a loading control. Representative western blots from three independent biological replicates are shown. B) Western blot data analysis of P4HA1, P4HA2, and PLOD2 expression on UT-SCC-7 cell line in monoculture. All experiments were repeated three times, and the results were shown in the mean±S.E.M value. C) Metastatic UT-SCC-7 cells were cocultured as 3D spheroids together with skin primary fibroblasts in both normoxia (21 % O_2) and hypoxia (3% O_2) for five days. The western blot method was used to analyze expressions of P4HA1, P4HA2, and PLOD2. β- tubulin was used as a loading control. Representative western blots from three independent biological replicates are shown. D) Western blot data analysis of P4HA1, P4HA2, and PLOD2 expression on UT-SCC-7 cells in coculture with skin fibroblasts. All experiments were repeated three times, and the results were shown in the mean±S.E.M value.

Results from RT3 cells showed that without fibroblasts, P4HA1 expression was downregulated in both hypoxia and normoxia in day 3 and day 5. However, expression was upregulated in day 1 in hypoxia compared to normoxia (Figure 15B). Interestingly, P4HA2 continued upregulation in hypoxia until day 3. However, collagen lysyl hydroxylase (PLOD2) was elevated in both normoxia and hypoxia conditions on day 5. The most profound upregulation was observed on day 3 in hypoxia (Figure 15B). Of note, changes in protein expressions were not statistically significant.

In RT3 cocultured spheroids, P4HA1 was upregulated in hypoxia compared to normoxia starting from day 1 to day 5. Two other ECM proteins, P4HA2 and PLOD2, were upregulated in normoxia on day 5. However, PLOD2 expression showed notable, albeit not significant, upregulation in hypoxia compared to normoxia on days 3 and 5 (Figure 15D). These results show that also in cocultured spheroids, containing transformed keratinocytes and fibroblasts, hypoxia increased the expression of the key enzymes in collagen biosynthesis and stabilization.

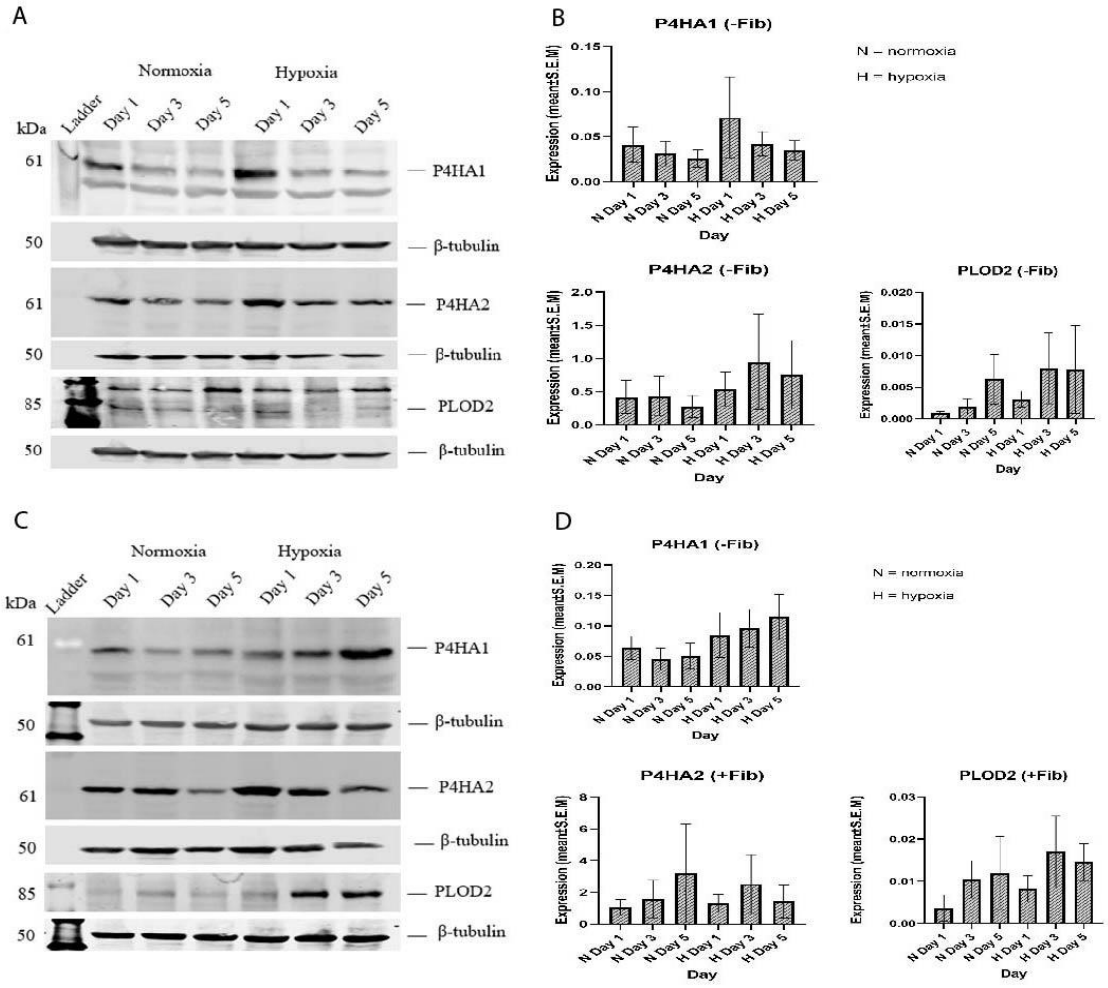

Figure 15. Expression of collagen prolyl hydroxylases (P4HA1 and P4HA2) and lysyl hydroxylase (PLOD2) expression in the H-Ras transformed keratinocyte (RT3). A) RT3 cells were cultured in 3D spheroids in monoculture in both normoxia (21 % O_2) and hypoxia (3 % O_2) for five days, and expressions of P4HA1, P4HA2, and PLOD2 were analyzed by western blot method. β-tubulin was used as a loading control. Representative western blots from three independent biological replicates are shown. B) Western blot data analysis of P4HA1, P4HA2, and PLOD2 expression on RT3 cell line in monoculture. All experiments were repeated three times, and the results were shown in the mean±S.E.M value. C) The RT3 cell line was cocultured in 3D spheroids together with skin primary fibroblasts in both normoxia (21 % O_2) and hypoxia (3% O_2) for 5 days. The western blot method was used to analyze expressions of P4HA1, P4HA2, and PLOD2. β- tubulin was used as a loading control. Representative western blots from three independent biological replicates are shown. D) Western blot data analysis of P4HA1, P4HA2, and PLOD2 expression on RT3 cell line in coculture. All experiments were repeated three times, and the results were shown in the mean±S.E.M value.

4.4 Elevated P4HA1 expression in hypoxia was observed by immunofluorescence assay

The effect of hypoxia on collagen protein (P4HA1) level was evaluated in cocultured spheroids by immunofluorescence staining. The cells were labelled in monolayer cultures with CellTrackers (RT3 cells with red and fibroblasts with green) to characterize the localization of different cell types. Then 3D spheroids were allowed to grow for 3 days, followed by staining with P4HA1 antibody.

The expression level of P4HA1 was compared both in normoxia and hypoxia conditions. The results showed that P4HA1 was highly expressed in hypoxia compared to the normoxia culture (Figure 16B). Confocal imaging also revealed that in normoxia, metastatic RT3 cells were in the periphery of the spheroid, whereas fibroblasts were located in the spheroid's center (Figure 16A). This is in accordance with previous results (Siljamäki *et al*., 2020). Furthermore, in normoxia, P4HA1 expression was most prominent in the core of the spheroids where also the fibroblasts locate. In contrast, in hypoxic condition P4HA1 expression and fibroblast localization were detected more in the periphery of the spheroids, whereas RT3 cells were located more throughout the spheroid (Figure 16B).

Confocal imaging results were verified by a computational analysis method. With this method, it is possible to analyze the expression profiles of the spheroids by considering different diameters and the intensity values of the spheroids. The expression profile of the spheroids cultured in normoxia showed that P4HA1 expression (magenta line) followed the profile of fibroblasts (green line) in the center of the spheroid (Figure 16C). In hypoxia, P4HA1 expression was shifted to the edge of the spheroid and fibroblast localization was more peripheral (Figure 16D).

Finally, intensity analysis of immunofluorescence images showed that P4HA1 expression was increased in hypoxia compared to normoxia in cocultured spheroids, as shown in Figure 16E. This result confirms that P4HA1 was highly increased in hypoxia compared to normoxia (Figure 16E).

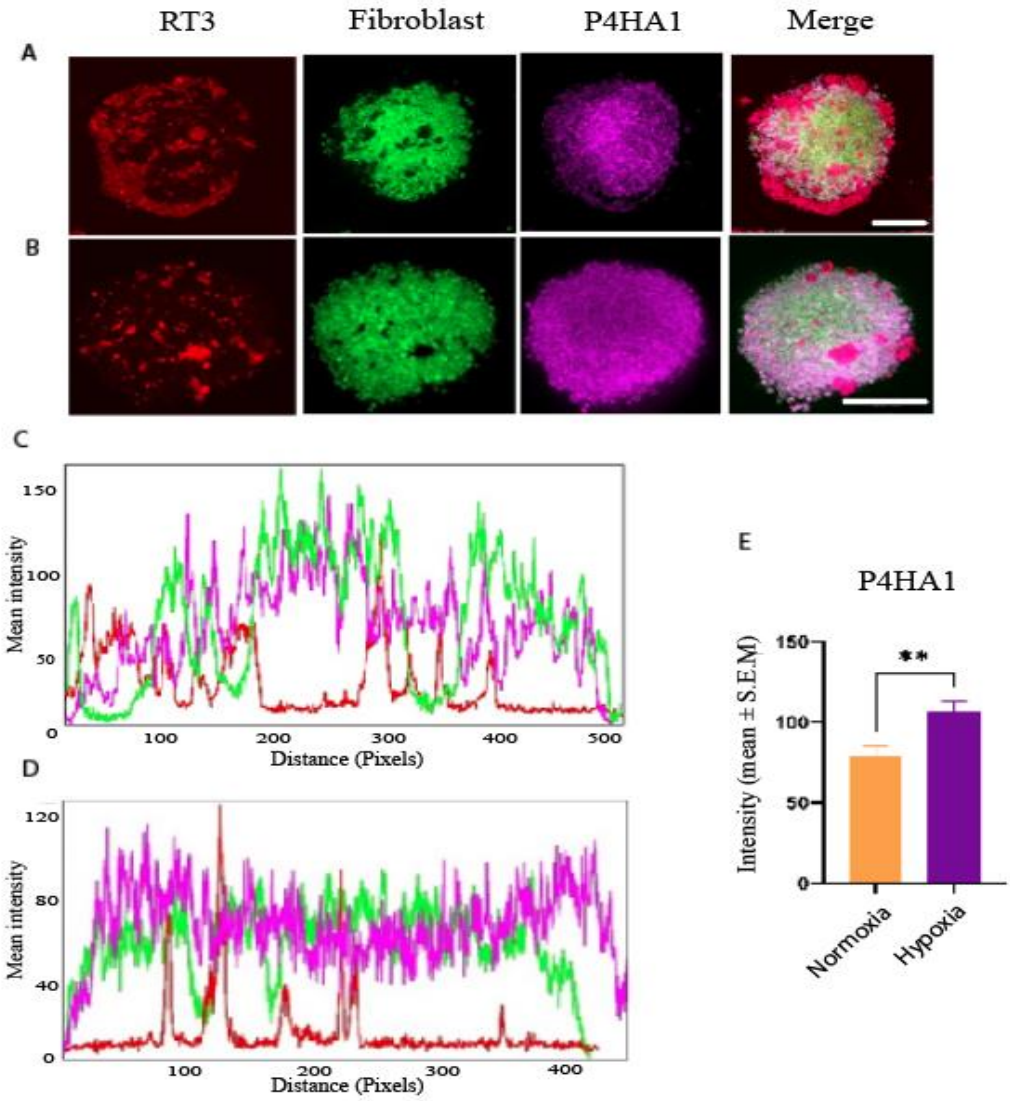

Figure 16. Hypoxia induces collagen prolyl hydroxylase (P4HA1) expression detected by immunofluorescence staining. A) Confocal images of RT3 3D spheroids cocultured with skin primary fibroblast in normoxia for three days. B) Confocal images of RT3 cells cocultured with skin primary fibroblasts in hypoxia for three days. CellTrackers were used to stain RT3 cells (in red) and fibroblasts (in green). P4HA1 is shown in magenta. Representative immunofluorescence images from one experiment (n=3 spheroids) are shown. Scale bar 200 µm. C, D) Intensity profile of 3D spheroids showing expression of RT3 (red), fibroblast (green), and P4HA1(magenta) in different positions of spheroids in normoxia (C) and hypoxia (D). Distances were measured by diameter using profile plot tools of ImageJ. E) P4HA1 intensity measurement of RT3+fibroblast spheroids in normoxia and hypoxia. The intensity profile was calculated from confocal images, and P4HA1 was significantly increased (*p*-value= 0.0061, n=3 spheroids, technical replicates) in hypoxia (Figure 16E). Intensity was shown in mean ± S.E.M.

4.5 Laminin-332 expression in 3D spheroids of UT-SCC-7 and RT3 cell lines in hypoxia and normoxia

Laminin-332 is a major protein component in the cutaneous basement membrane. Previously it has been shown that hyperactive H-Ras and stromal fibroblast-related induction in TGF-β signaling co-operate in the synthesis of laminin-332 in cSCC. Very recently, laminin-332 synthesis has also been shown to be regulated by TGF-β-activated p38 signaling in cSCC (Siljamäki *et al*., 2022). To investigate laminin-332 expression in hypoxic (3% O_2) and normoxic (21% O_2) conditions, UT-SCC-7 cells and RT3 cells were cultured as 3D spheroids with or without skin primary fibroblasts. The spheroids were allowed to grow for one to six days before harvesting for western blotting. Possible changes in signaling pathways regulating laminin-332 synthesis in normoxia versus hypoxia were also investigated.

The results showed that without fibroblasts, laminin α3 and β3 chain expressions were upregulated on day 1 in UT-SCC-7 monocultures in hypoxic conditions compared to normoxic conditions (Figure 17A, B). However, γ2 chain expression was slightly decreased in hypoxia at all time points compared to normoxic conditions. Expressions of phosphorylated ERK1/2 (p-ERK1/2) and phosphorylated CREB (p-CREB; downstream target of p38 signaling) in hypoxia were downregulated at all time points compared to normoxia, but there was no change in the expression of p-Smad2 (Figure 17B). These results suggest that the decrease in γ2 chain expression in monocultured UT-SCC-7 cells in hypoxia could be caused by the downregulation of Ras and p38 signaling. When UT-SCC-7 cells were cocultured with fibroblasts, β3 chain was upregulated in day 4 both in normoxia and in hypoxia. Results also revealed that in hypoxic conditions, γ2 chain expression was slightly, but not significantly, upregulated in day 4 (Figure 17D). Interestingly, compared to normoxia, in hypoxia p-ERK1/2 and p-Smad2 expressions were downregulated on day 1, and p-CREB expression was downregulated starting from day 4. These results suggest that in UT-SCC-7 cocultures, inhibition of laminin-332 γ2 chain expression in hypoxia might be due to the downregulation of Ras and TGF-β signaling pathways. In later time points also decrease in p38 signaling might contribute to γ2 chain expression inhibition. However, the results are non-significant.

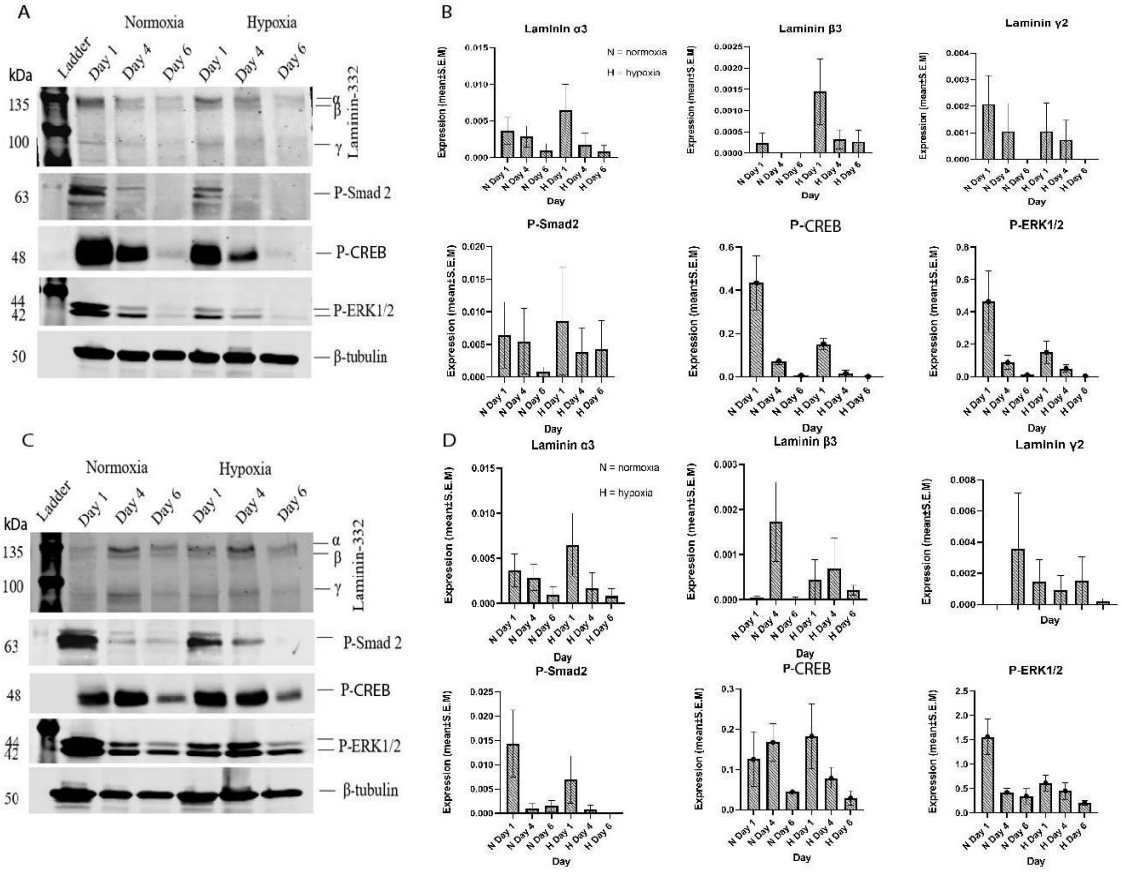

Figure 17. Laminin-332 expression in UT-SCC-7 cells. A) Metastatic UT-SCC-7 cell line was cultured as 3D spheroids in monoculture in both normoxia (21 % O_2) and hypoxia (3 % O_2) for 6 days, and the levels of laminin-332, p-Smad2, p-CREB and p-ERK1/2 were analyzed by western blot method. β-tubulin was used as a loading control. Representative western blots from three independent biological replicates are shown. B) Western blot data analysis of laminin-322 (α, β, γ chains), p-ERK1/2, p-CREB, and p-Smad2 expression on UT-SCC-7 cell monoculture. All experiments were repeated three times, and the results were shown in the mean±S.E.M value. C) UT-SCC-7 cells were cocultured as 3D spheroids with skin primary fibroblasts in both normoxia (21 % O_2) and hypoxia (3 % O_2) for six days, and the levels of laminin-332, p-Smad2, p-CREB, and p-ERK1/2 were analyzed by western blot method. β-tubulin was used as a loading control. Laminin α3, β3, and γ2 chains are also separately marked in the Figure. Representative western blots from three independent biological replicates are shown. D) Western blot data analysis of laminin-322 (α, β, γ chains), p-ERK1/2, p-CREB, and p-Smad2 expression on UT-SCC-7 spheroids with fibroblasts. All experiments were repeated three times, and the results were shown in the mean±S.E.M value.

In RT3 monocultures, the result showed that laminin α3, β3 were downregulated on day 4, 6, and γ2 chain on day 6 in hypoxia compared to normoxia, however these chains were upregulated gradually from day 1 to 6 in normoxia (Figure 18A, B). Expression of p-CREB was downregulated in hypoxia only on day 6, however expression levels of p-ERK1/2 and p-Smad2 were downregulated in all time points in hypoxia compared to normoxia. These results suggest that also in RT3 monocultures, laminin-332 downregulation in hypoxia might be caused by inhibition of TGF-β and Ras signaling pathways in the earlier time points, and in later time points also p38 signaling downregulation may contribute to the attenuation of laminin-332 synthesis.

In RT3 cocultured spheroids, laminin α3, β3, and γ2 chain levels were upregulated in day 4 and day 6 in normoxia, but they were remarkably downregulated in hypoxia during the same time points (Figure 18C, D). Also p-Smad2 and p-ERK1/2 expression levels were downregulated in hypoxia in all time points and p-CREB expression was decreased on day 6 compared to normoxia (Figure 18C, D). These results suggest that like in monocultures, also in cocultures the downregulation of laminin-332 synthesis in hypoxia could be due to downregulation in TGF-β and Ras signaling pathways and in later time points also due to p38 signaling inhibition.

Unexpectedly, p-Smad2 expression was downregulated in normoxia on days 4 and 6 both in RT3 monocultures and cocultures with fibroblasts, while laminin-332 synthesis was increased. Previously it has been shown that both hyperactive Ras and TGF-β signaling are needed for laminin-332 upregulation in RT3 cells (Siljamäki *et al*., 2020). Here, deviations between experiments are high and thus the result is not statistically significant. Thus, this result need further verification.

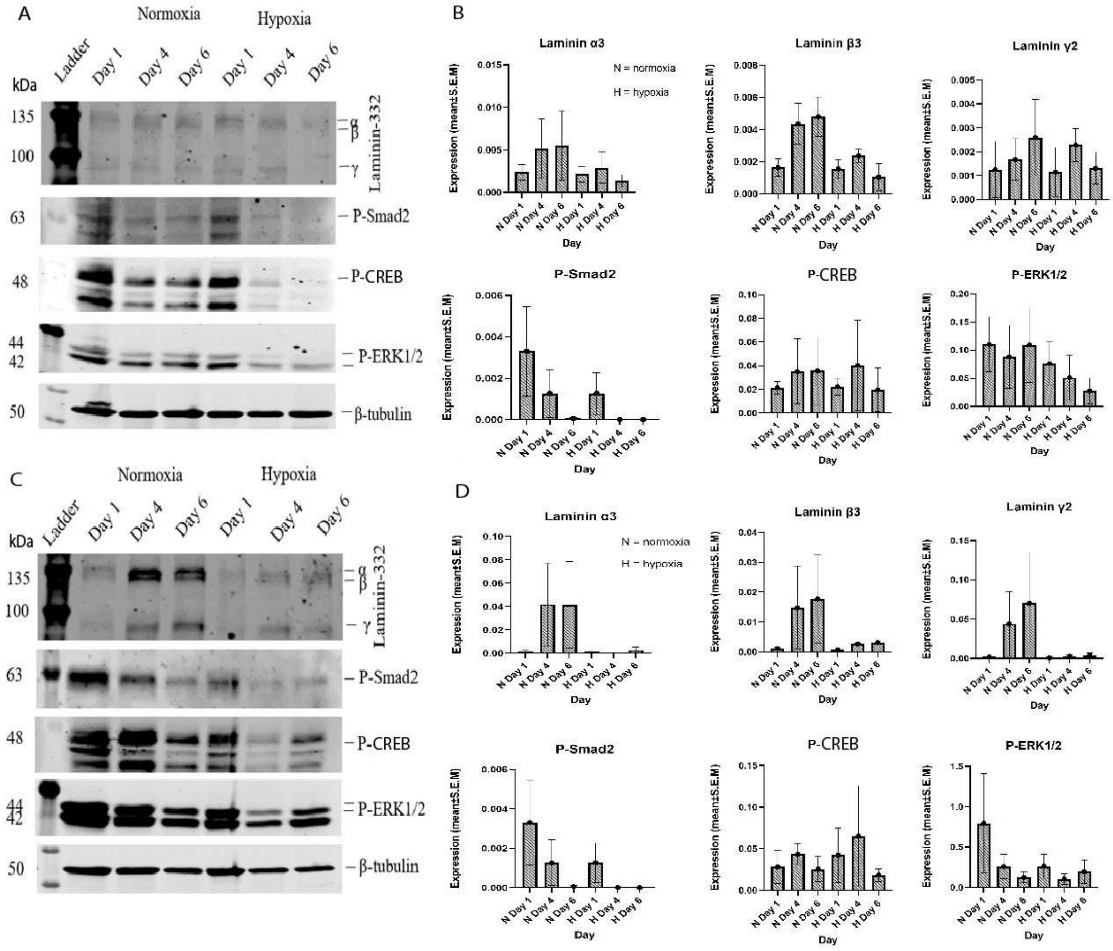

Figure 18. Laminin-332 expression in RT3 spheroids. A) RT3 cell line was cultured as 3D spheroids in monoculture in both normoxia (21 % O_2) and hypoxia (3 % O_2) for 6 days, and the levels of laminin-332, p-Smad2, P-CREB and p-ERK1/2 were analyzed by western blot method. β-tubulin was used as a loading control. Representative western blots from three independent biological replicates are shown. B) Western blot data analysis of laminin-322 (α, β, γ chains), p-ERK1/2, p-CREB, and p-Smad2 expression on RT3 cell monoculture. All experiments were repeated three times, and the results were shown in the mean±S.E.M value. C) RT3 cell line was cocultured as 3D spheroids with skin primary fibroblast in both normoxia (21 % O_2) and hypoxia (3 % O_2) for six days, and the levels of laminin-332, p-Smad2, p-CREB and p-ERK1/2 were analyzed by western blot method. β-tubulin was used as a loading control. Representative western blots from three independent biological replicates are shown. D) Western blot data analysis of laminin-322 (α, β, γ chains), p-ERK1/2, p-CREB, and p-Smad2 expression on RT3 cells with fibroblasts. All experiments were repeated three times, and the results were shown in the mean±S.E.M value.

4.6 Mass spectrometry analysis of 3D spheroids cultured in hypoxia and normoxia

Mass spectrometry (MS) was performed to analyze total ECM proteins in the 3D spheroids formed by UT-SCC-7 and RT3 cancer cells in monoculture and coculture conditions. In addition, 3D spheroids generated from only skin fibroblasts were also analyzed.

The results obtained from MS analysis showed a total of 193 ECM proteins. In addition, several ECM proteins upregulated by fibroblasts were detected. In accordance with western blot results, P4HA1, P4HA1, and PLOD2 expressions were highly upregulated in coculture in hypoxia, and a slight upregulation of these proteins was also seen in monocultures in hypoxic conditions (Figure 19). On the other hand, spheroids formed solely by fibroblasts showed higher expression of these three proteins in both normoxia and hypoxia. Also, laminin-332 expression in UT-SCC-7 spheroids followed the results obtained from western blots. However, in cocultured UT-SCC-7 spheroids in hypoxia, the β3 and γ2 chain expressions (LAMB3 and LAMC2, respectively) were downregulated. The most prominent downregulation was seen in the α3 chain (LAMA3). In contrast, cocultured RT3 cells showed increased α3, β3, and γ2 chain expressions in hypoxia compared to normoxia (Figure 19).

In addition, PLOD3, a collagen lysyl hydroxylase, was also upregulated in UT-SCC-7 cocultures with fibroblasts in hypoxia compared to normoxia (Attachment figure 3A). Other essential ECM proteins, for example matrix metalloproteinase-1 (MMP-1) was also upregulated in hypoxia in RT3 and UT-SCC-7 cocultures with fibroblasts. Also, protein TNFα stimulated gene-6 (TSG6) was upregulated in RT3 and UT-SCC-7 cocultures with fibroblasts in hypoxia. In addition, synthesis of MMP-10 and type VI collagen (COL6) were elevated in samples containing UT-SCC-7 cells and fibroblasts in hypoxia (Attachment figure 3A and 3B). These results show that fibroblasts have a significant role in modulating the synthesis of various ECM components in hypoxia.

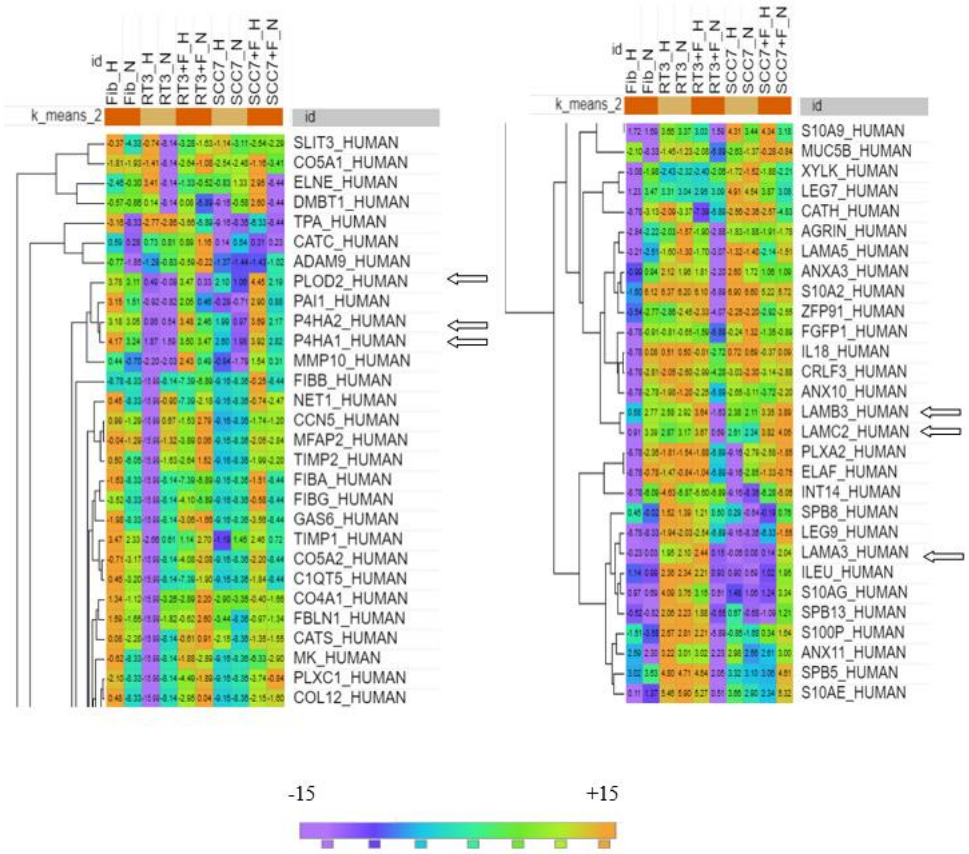

Figure 19. Mass spectrometric analysis of 3D spheroids of RT3 and UT-SCC-7 cells in monocultures and cocultures with skin primary fibroblasts. Fibroblasts were also monocultured as 3D spheroids. H=hypoxia; N=normoxia. Arrows show collagen prolyl hydroxylases (P4HA1, P4HA2) and lysyl hydroxylase (PLOD2). Also, three chains of laminin-332, i.e. LAMA3 (α3 chain), LAMB3 (β3 chain), and LAMC2 (γ2 chain) are pointed by arrows. One number difference (Matrisome-only values) in MS results between two samples means twice the expression difference.

5. DISCUSSION

ECM is an essential component in the tumor microenvironment and plays a critical role in cancer progression and metastasis (Balkwill *et al*., 2012). ECM proteins are strongly associated with and remodeled by hypoxia. Indeed, hypoxia is common in the majority of solid tumors, and the phenomenon causes resistance to cancer treatment and relapse (Ham *et al*., 2016; Muz *et al*., 2015). Studies have shown that cancer cells subjected to hypoxia result in cell adaptation, survival, and malignant potential (Emami Nejad *et al*., 2021; Vinaiphat *et al*., 2021)**.** However, the role of hypoxia on ECM protein regulation in cancer has not yet been fully understood. Our current study was driven by the underlying of this principle; effects of hypoxia in cSCC in regulating ECM proteins, remodeling, and cancer metastasis (Gilkes *et al*., 2013a).

cSCC is a non-melanoma skin cancer, one of the most lethal among all skin cancers. Previously it has been demonstrated that laminin-332, which is an essential glycoprotein in the basement membrane, is one of the driving factors in cSCC invasion (Siljamäki *et al*., 2020). This study explored whether laminin-332 and other ECM proteins, such as collagen, are differently regulated in hypoxia compared to normoxia in our 3D spheroid model.

Despite of surgical excision, resistance to treatment is a significant obstacle that inevitably underlies uncontrolled tumor recurrence. There is an unmet need to discover novel, effective new diagnostics methods for cSCC. Previous studies have screened that the cancer 3D spheroids model is an indispensable method for cancer diagnosis and treatment (Boucherit *et al*., 2020) as it resembles the tumor microenvironment *in vivo* (Edmondson *et al*., 2014). Fibroblasts, cells that produce the majority of the ECM proteins, could be included in the 3D spheroids model, in contrast to the conventional 2D cell culture method. Previously it has been also demonstrated that some proteins are expressed only in 3D spheroids and not in 2D culture (Y. E. Kim *et al*., 2018). Hence, 3D spheroids could be a promising tool for cancer cell biology research and drug discovery and development in the future.

5.1 Cellular response to hypoxia in 3D spheroids

In the beginning of this study we explored how cancer cell proliferation is affected by hypoxia. In hypoxia (3% O_2), it was found that the cell proliferation rate was faster compared to normoxia both in monocultured RT3 cells and in coculture with skin fibroblasts. Previous studies have shown that DNA synthesis is elevated in hypoxia in response to bFGF and PDGF in vascular wall cells in rats (Humar *et al*., 2002). Also, hypoxia could either increase autophagy activation or halt the cell cycle's G1 phase, leading to cell adaptation or survival even under cancer therapy (Qiu *et al*., 2015). Furthermore, it has been demonstrated that hypoxia significantly increases proliferation in mesenchymal stem cells in 5% O_2 (Kwon *et al*., 2017).

Cell proliferation was also visible in morphology analysis. In monocultured RT3 and UT-SCC-7 spheroids, typical spheroid zones were not properly visible. However, as expected, tight spheroids were formed in cocultures with skin primary fibroblasts, and all three zones such as necrotic core, quiescent zone, and proliferative zone were divisible in day 6 both in normoxia and in hypoxia. The morphology of the spheroids follows previously reported results (Siljamäki *et al*., 2020) and thus confirms that our 3D spheroid model worked well both in normoxic and hypoxic conditions.

5.2 Hypoxia induces collagen deposition and cross-linking in the ECM

The current study sought to investigate the role of hypoxia on ECM protein regulation in the 3D spheroid model. We investigated the protein expression of two isoforms of collagen prolyl hydroxylase (P4HA1, P4HA2) and lysyl hydroxylase (PLOD2) in hypoxia in 3D spheroids culture. There is mounting evidence that hypoxia regulates collagen prolyl hydroxylases and lysyl hydroxylase, two of collagen modifying enzymes. P4HA1, P4HA2, and PLOD2 are found to be highly expressed in different cancers, such as lung adenocarcinoma, clear cell renal cell carcinoma, breast cancer, and cervical cancer (Gilkes *et al*., 2013a; Li *et al*., 2022; Robinson *et al*., 2021; Yang *et al*., 2021). Furthermore, collagen-modifying enzymes were found to be increased in hypoxia in breast cancer (Gilkes *et al*., 2013a). However, these enzymes are required for collagen fiber formation and cross-linking with elastin in hypoxia (Gilkes *et al*., 2013a; Xiong *et*

al., 2018). Our study found that collagen P4HA1, P4HA2, and PLOD2 synthesis were highly elevated, although not significantly, in hypoxia compared to normoxia in both UT-SCC-7 and RT3 spheroids. This suggests that collagen prolyl hydroxylase might be responsible for collagen fiber formation, and consequently, collagen deposition in hypoxia in our 3D model system.

Collagen biogenesis includes exclusive post-translational modification. Previous studies have confirmed that lysine hydroxylation is one of the post-translational modification processes involved in collagen cross-linking. Moreover, cross-linking through hydroxylation is more stable than cross-linking derived from lysis. Therefore, we have used collagen lysyl hydroxylase (PLOD2), specific telopeptide of procollagen. However, future studies could include also PLOD1, as PLOD1 hydroxylases α-helical or central domain (Gilkes *et al*., 2013b; Lu *et al*., 2011). Unlike P4HA1 and P4HA2 knockdown, PLOD2 knockdown has been shown to reduce collagen stiffness and fibrillar collagen formation (Gilkes *et al*., 2013b), which suggests that also in our study, increased expression of PLOD2 in hypoxia is responsible for collagen crosslinking as well as stiffness, and finally ECM remodeling. It is also notable that we have used L ascorbic acid (vitamin C) in culture media, as it is essential for collagen biogenesis. It is reported that, L ascorbic acid is a cofactor for prolyl hydroxylase and lysyl hydroxylase and stimulates biosynthesis of procollagen (Pinnel *et al*., 1987; Pinnell, 1985).

Also, remarkable increase in expression of these three enzymes was perceived when fibroblasts were added to the spheroids with either UT-SCC-7 or RT3 cell lines. Several *in vitro* studies have shown that fibroblasts, more specifically CAFs, are the most significant stromal cells responsible for ECM remodeling in cancer (Li *et al*., 2021; Mhaidly & Mechta-Grigoriou, 2020). It was previously assessed that fibroblasts control other cells and tumor progression by producing ECM proteins and growth factors. Hence, fibroblasts' association with cancer cells lead to tumor growth, invasion, and chemoresistance (D'Arcangelo *et al*., 2020; Friedman *et al*., 2020). Also, we show here that in our 3D spheroid model fibroblasts in coculture with cancer cells are inducing the production of these proteins (P4HA1, P4HA2, and PLOD2).

5.3 Immunofluorescence staining has confirmed elevated P4HA1 expression in H-RAS transformed keratinocytes of cocultured 3D spheroids

The present study assessed collagen prolyl hydroxylase (P4HA1) expression in hypoxia and normoxia using immunofluorescence staining and confocal imaging. P4HA1 expression was increased in hypoxia compared to normoxia condition. Results from previous studies, performed using conventional 2D methods, correlate with the findings of our current study (Gilkes *et al*., 2013a; Yang *et al*., 2021; Zhang *et al*., 2021). Thus, our results demonstrate that we have successfully created a 3D spheroid model that could not only reproduce results from 2D cell culture but could also better mimic actual tumors. It was also previously demonstrated that P4HA1 stabilize HIF-1α, which is a key transcription factor in hypoxia (Xiong *et al*., 2018; Zhang *et al*., 2021). In addition, localization analysis of P4HA1 in cocultured RT3 spheroids was performed. We detected that in normoxia, P4HA1 was located in the central part of the 3D spheroids, associated with fibroblasts. This suggests that fibroblasts were responsible for collagen deposition in the ECM. In contrast, RT3 cells were located in the outer part of the spheroids which is in accordance with previous results (Siljamäki *et al*., 2020). In hypoxia, P4HA1 expression was shifted to the edges of the spheroids, and the localization of fibroblasts was more spread compared to normoxia. RT3 cells showed more spread localization compared to normoxic condition. Altogether our results demonstrate that also by immunofluorescence approach, our 3D spheroid model shows increased P4HA1 synthesis in hypoxia, and we also confirm that its expression follows fibroblast localization. As the experiment was conducted only once due to limited time, it would be useful to confirm the result of the immunofluorescence staining with more biological repeats.

Finally, P4HA1 expression from three spheroids was determined by intensity measurement, confirming an increase in P4HA1 expression in hypoxia. In future, different cancer cell lines could be studied to assess the expression of collagen under hypoxic condition.

5.4 Laminin-332 expression in hypoxia

In the current study, laminin was also studied along with collagen, as laminin-332 is a prominent glycoprotein in cSCC carcinoma. Previously it has been demonstrated that hypoxia produces laminin rich matrix in immortalized breast epithelial cells (Vaapil *et al*., 2012). In addition, we investigated some of the signaling pathways regulating laminin-332 synthesis. In our western blot results, we could differentiate three chains of laminin-332 in both normoxia and hypoxia. Rousselle and colleagues have demonstrated that different laminin-332 cleavage products can be found in cancer cells, for example, α3β3γ2(cleavage), β3γ2 dimer, γ2 monomer and cleaved α3 (Rousselle & Scoazec, 2020). Our results showed that in hypoxic conditions, both in monocultured and cocultured UT-SCC-7 spheroids laminin γ2 chain expression was downregulated. Along with γ2 downregulation, also decrease in Ras and p38 signaling pathways (in monocultures) and in Ras and TGF-β signaling pathways (in cocultures) was apparent. These results are in accordance with previous results showing that laminin-332 synthesis is regulated by hyperactive Ras and TGF-β pathways, and by TGF-β activated p38 signaling pathway (Siljamäki *et al*., 2022; Siljamäki *et al*., 2020). In the case of RT3 cells, all the laminin chains (α3, β3 and γ2) were downregulated in hypoxia both in monocultured and cocultured spheroids. TGF-β and Ras signaling pathways were also attenuated in the earlier time points, and in later time points also p38 signaling was downregulated. Of note, our western blot results were not statistically significant and thus these results need further verification before strong conclusions of laminin-332 regulation in hypoxia in cSCC can be made.

Previously it has been demonstrated that chronic mild hypoxia increases laminin-111 and -411 expression; however, the experiment was addressed in the blood-brain barrier and in 2D cell culture condition (Halder *et al*., 2018). Interestingly, it has been shown that when human keratinocytes were exposed to acute hypoxia, secretion of laminin-332 was significantly inhibited (O'Toole *et al*., 1997). Conversely, human corneal epithelial cells produce less laminin-332 and become apoptotic in chronic hypoxia after day 7 (Esco *et al*., 2001). Thus, further research is needed to clarify changes in laminin, and especially laminin-332, expression in hypoxic condition.

Some experiments have demonstrated that hypoxia upregulates p38/ERK signaling in hepatocellular carcinomas (Chen *et al*., 2018), but it has also been documented that p38 phosphorylation decreases in hypoxia in lung epithelial cells (Powell *et al*., 2004). HIF-2α has been shown to promote human placenta-derived mesenchymal stem cell proliferation via MAPK/ERK signaling pathway (Zhu *et al*., 2016) and hypoxia has been shown to enhance for example periodontal ligament stem cell proliferation via MAPK signaling pathway (He *et al*., 2016). However, also opposite results have been found. In mouse embryonic stem cells ERK was dephosphorylated in 1% O_2 (Kučera *et al*., 2017).

TGF-β signaling is often activated during hypoxia and promotes cancer. Multifunctional TGF-β is responsible for angiogenesis, and immune suppression in many cancers (Mallikarjuna *et al*., 2022). For example, long term exposure to hypoxia leads to TGF-β activated Smad2 phosphorylation in lung cancer (Furuta *et al*., 2015). These are contradictory to our result, as we show that Smad2 phosphorylation was decreased in hypoxia. However, in our experiments, downregulation of TGF-β signaling could possibly explain the observed decrease in laminin-332 synthesis. Interestingly, TGFBR2 expression has been shown to be decreased in hypoxic condition in prostate cancer (Zhou *et al*., 2018). Changes in TGF-β signaling in hypoxic condition can therefore be context-dependent and need further research.

5.5 Mass spectrometry analysis in 3D spheroids

In hypoxia, heterogenic cancer cell population and disruption of cellular mechanism make it challenging to target a single protein for cancer treatment. Mass spectrometry (MS) makes it possible to analyze single protein levels and observe how they are regulated in different conditions. To analyze possible hypoxia-induced ECM proteins, MS was performed of cocultured 3D spheroids of RT3 and UT-SCC-7 cells with skin primary fibroblasts. Also monocultured fibroblasts, RT3 and UT-SCC-7 cells were included in the analyses. Our result presents the matrisome of UT-SCC-7 and RT3 cells in normoxia and hypoxia conditions. A total of 193 ECM proteins were found in all samples. Proteins were selected if they have at least two peptides present. Proteins involved in oxidoreductase activity, for example, P4HA1, P4HA2, and PLOD2, were found to be enriched in both coculture and monoculture. That is also correlated with the previous

studies (Bousquet *et al*., 2015). Therefore, it could be postulated that upregulation of these proteins in hypoxia is involved in ECM remodeling. Another candidate of ECM protein, laminin-332, separately its α3 (LAMA3), β3 (LAMB3), and γ2 (LAMA2) chains were found to be decreased in hypoxia in UT-SCC-7 coculture, which supports our western blot results. However, when RT3 cells were cocultured with fibroblasts, laminin-332 expression was higher in hypoxia compared to normoxia. On the other hand, monocultured fibroblast spheroids showed downregulation of laminin-332 in hypoxia. Possible changes in regulation of laminin-332 synthesis in hypoxia needs further verification and additional experiments.

We also found that a tissue inhibitor of metalloproteinase 3 (TIMP3) was upregulated in cocultures in hypoxia. In previous studies, TIMP3 has been found only *in vitro* (Ojalill *et al*., 2018). This suggests that fibroblasts *in vitro* exclusively remodel ECM in hypoxia. In addition to TIMP3, MMP1 was upregulated in hypoxia in RT3 and UT-SCC-7 cocultures with fibroblasts. It has been reported that MMPs are induced in hypoxia in chondrosarcoma cell invasion via ERK signaling (Sun *et al*., 2010). In addition, in our MS analysis, Protein TNFα stimulated gene-6 (TSG6), which is a ECM remodeling protein and activated through ERK signaling, was found to be upregulated in RT3 and UT-SCC-7 cocultures in hypoxia (Liu *et al*., 2022). We also found that FGF-2 was upregulated in monocultured fibroblast spheroids in hypoxia. FGF-2 is a protein which plays role in tissue repairing (Prudovsky, 2021) and it is suggested that FGF-2 is one of the key players in cell proliferation in hypoxia. However, it was also reported that FGF-2 was available only *in vitro*, not *in vivo* (Ojalill *et al*., 2018). It is worth to notice that we performed the mass spectrometry analysis only once. So further repetition and investigation is mandatory before strong conclusions can be made. Molecular mechanism disruption due to hypoxia is a critical factor in cancer therapy. Some of the hypoxia-selective cytokines and drugs are already in the trial phage. However, these drugs did not get maximum therapeutic effects (Vinaiphat *et al*., 2021). In this regard, selecting a single protein and its regulation in hypoxia, along with hypoxia-associated *in vitro* culture method development like 3D spheroids, may lead to successful hypoxia-targeted therapy.

6. CONCLUSIONS AND FUTURE PERSPECTIVES

Extracellular protein remodeling due to hypoxia and activation of cancer-associated fibroblasts have been proposed to contribute to cancer progression and metastasis. From this current study, we have gained insight into the pattern of ECM protein synthesis in hypoxia and the sensitivity of the 3D spheroids model. This study demonstrates the following findings,

i. Hypoxia induces cell proliferation of cancer cells in monoculture and coculture of 3D spheroids.

ii. Collagen prolyl hydroxylases and lysyl hydroxylases are key modulators of collagen synthesis and responsible for ECM remodeling during hypoxia. Increased expression of collagen prolyl hydroxylases and lysyl hydroxylase in hypoxia compared to normoxia was confirmed.

iii. Fibroblasts are responsible for collagen deposition in 3D spheroids model *in vitro.*

iv. Downregulation of laminin-332 in hypoxia still needs further investigation.

v. Finally, these results suggest that the results of our 3D coculture method correlate with *in vivo* results in ECM protein modulation

Understanding of ECM remodeling in hypoxic condition is essential as the remodeling can lead to cancer metastasis. Also, ECM itself is a reservoir of growth factors. Our results demonstrate that fibroblasts, which are the main source of ECM proteins in tumor stroma, gets activated in hypoxia. We also show increase in several hypoxia-related protein expressions. In future studies, we could include HIF-1 inhibitors, potential anticancer drugs, to test in our 3D spheroid model. We could also work with HIF/LOX signaling pathways as they are considered as therapeutic targets to suppress collagen remodeling and crosslinking. As laminin-332 was downregulated in hypoxia in cSCC, we could use other cancer cell types in our 3D spheroid model that could give more insight into the laminin-332 synthesis and sensitivity of this model when detecting changes in ECM protein levels in hypoxia.

APPENDICES

1. Confocal images of H-Ras transformed keratinocytes (RT3) cocultured as 3D spheroids with skin primary fibroblasts in normoxia, and profile plot analysis of localization.

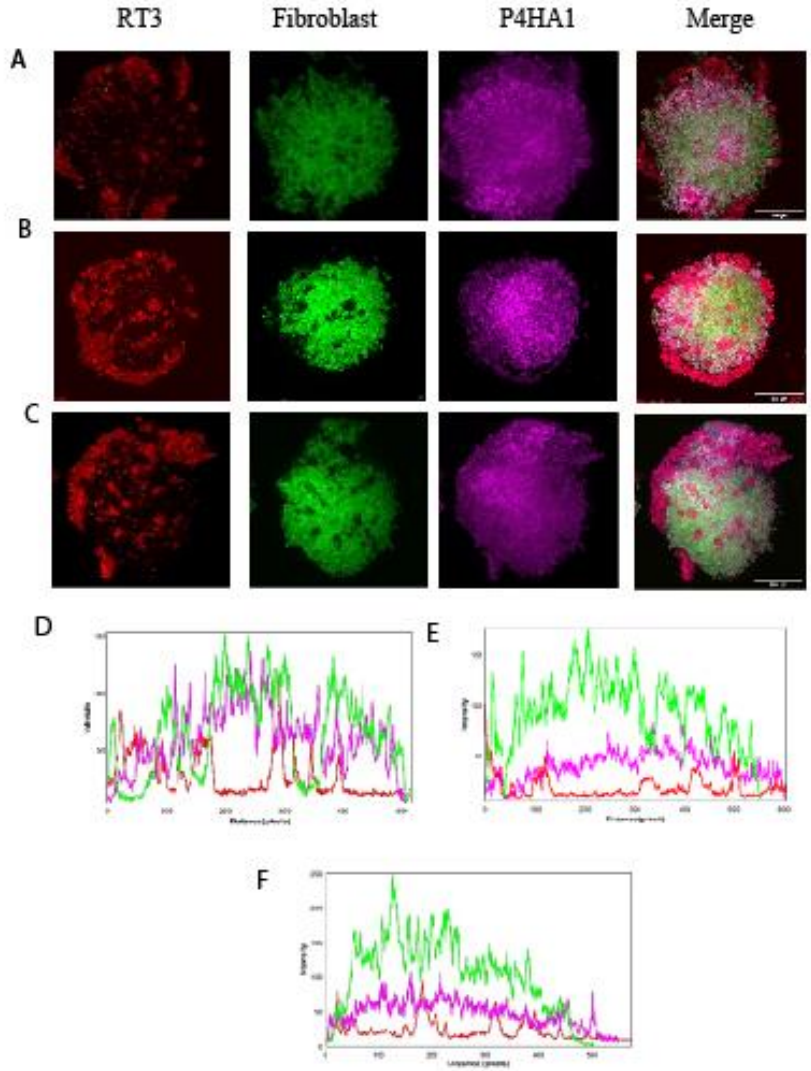

Attachment figure 1. A, B, C) Confocal images of three different RT3+fibroblast spheroids cultured in normoxia for three days. D, E, F) Intensity (mean intensity) profile plots of RT3 cells (red), fibroblasts (green) and P4HA1 (magenta) shows the localization of the different cell lines and P4HA1 in the spheroids. The profile plots D, E and F are created from the spheroids in A, B and C, respectively.

2. Confocal images of H-Ras transformed keratinocytes cocultured 3D spheroids in hypoxia and profile plot analysis of localization.

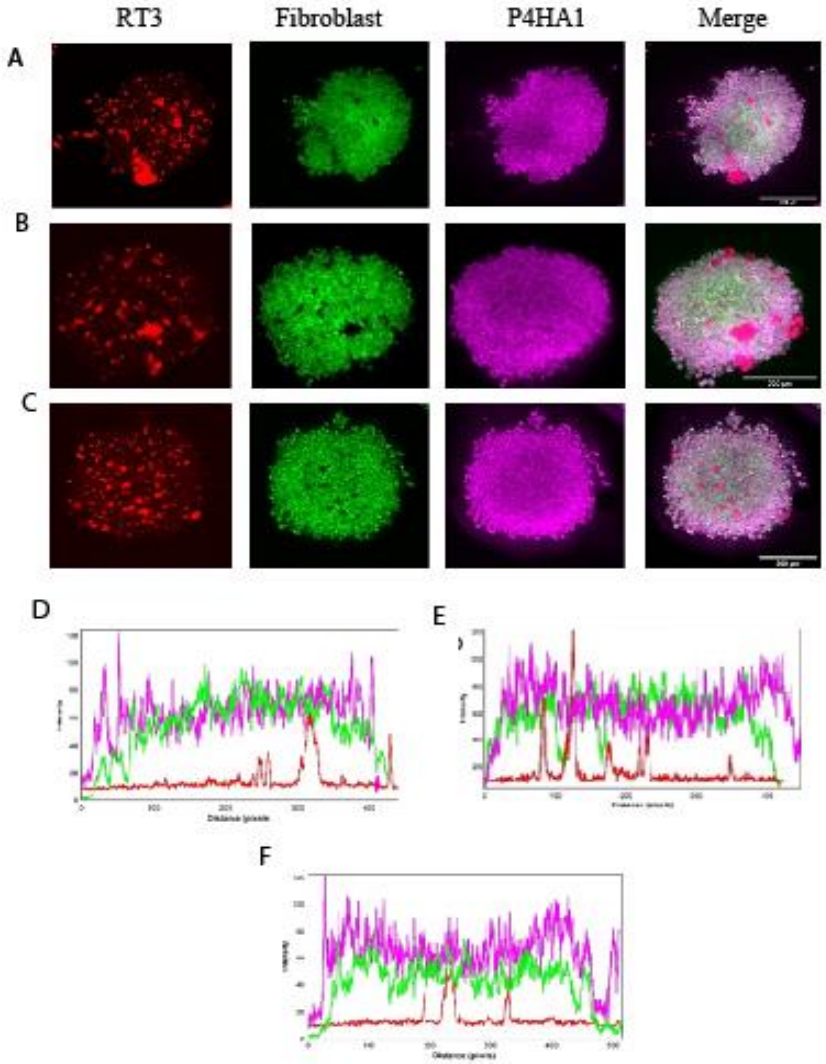

Attachment figure 2. A, B, C) Confocal images of three different RT3+fibroblast spheroids cultured in hypoxia for three days. D, E, F) Intensity (mean intensity) profile plots of RT3 cells (red), fibroblasts (green) and P4HA1 (magenta) shows the localization of the different cell lines and P4HA1 in the spheroids. The profile plots D, E and F are created from the spheroids in A, B and C, respectively.

3. Mass spectrometry analysis of total ECM protein in normoxia and hypoxia.

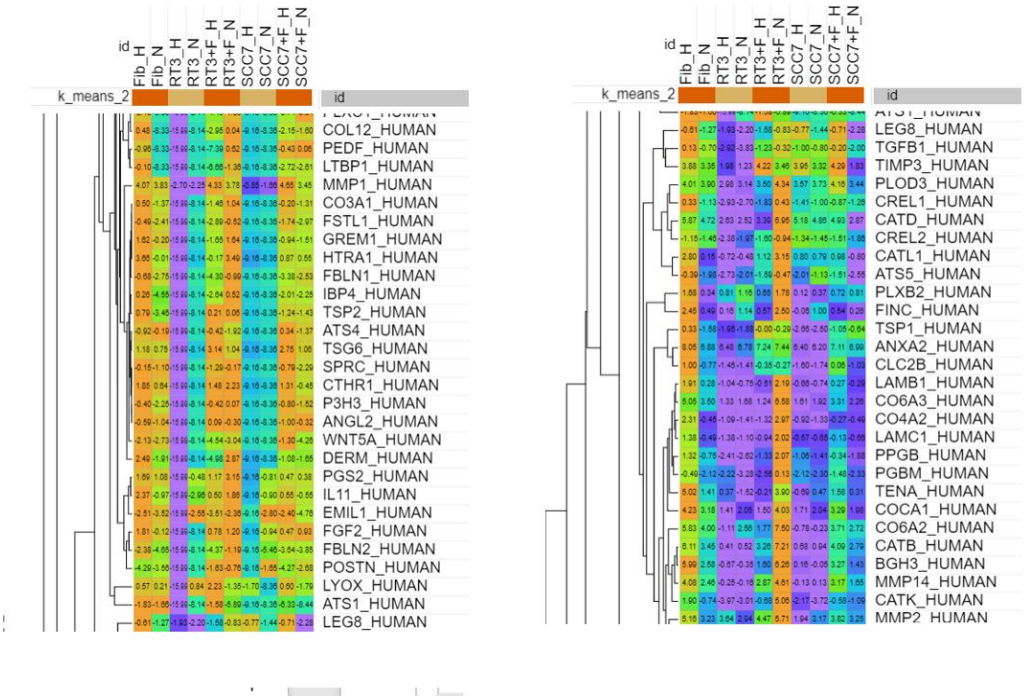

Attachment figure 3A. Mass spectrometric analysis of 3D spheroids of skin primary fibroblasts alone, and RT3 cells and UT-SCC-7 cells in monoculture and coculture with skin primary fibroblasts in hypoxia (H) and normoxia (N).

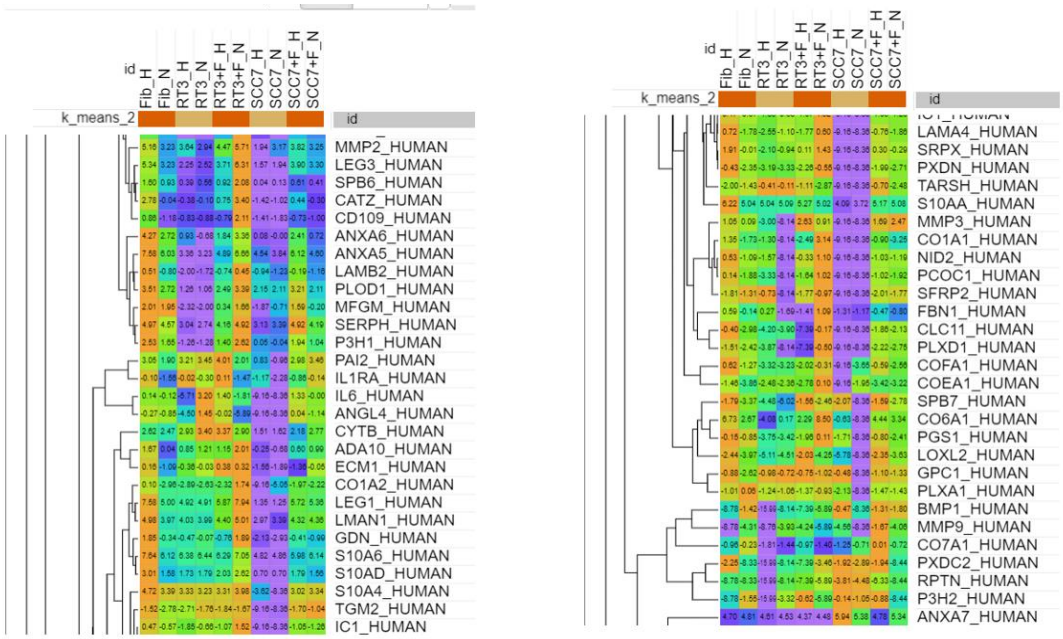

Attachment figure 3B. Mass spectrometric analysis of 3D spheroids of skin primary fibroblasts alone, and RT3 cells and UT-SCC-7 cells in monoculture and coculture with skin primary fibroblasts in hypoxia (H) and normoxia (N).

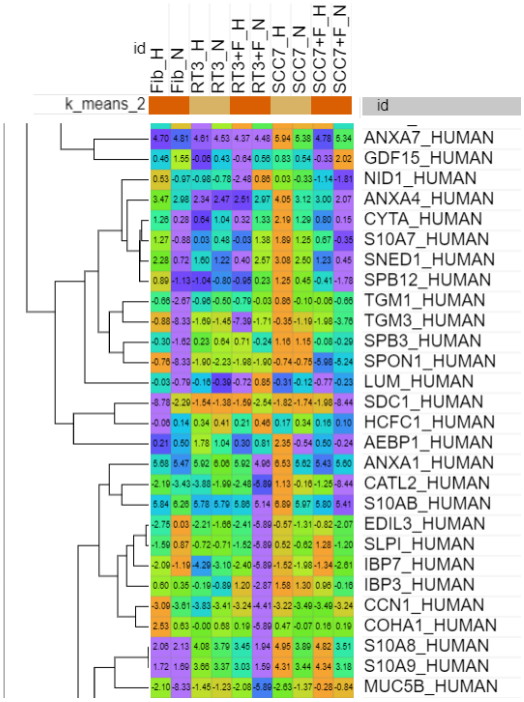

Attachment figure 3C. Mass spectrometric analysis of 3D spheroids of skin primary fibroblasts alone, and RT3 cells and UT-SCC-7 cells in monoculture and coculture with skin primary fibroblasts in hypoxia (H) and normoxia (N).

REFERENCES

Annunen, P., Autio-Harmainen, H., & Kivirikko, K. I. (1998). The novel type II prolyl 4-hydroxylase is the main enzyme form in chondrocytes and capillary endothelial cells, whereas the type I enzyme predominates in most cells. *The Journal of Biological Chemistry*, **273**, 5989–5992.

Aro, E., Khatri, R., Gerard-O'Riley, R., Mangiavini, L., Myllyharju, J., & Schipani, E. (2012). Hypoxia-inducible Factor-1 (HIF-1) but Not HIF-2 Is Essential for Hypoxic Induction of Collagen Prolyl 4-Hydroxylases in Primary Newborn Mouse Epiphyseal Growth Plate Chondrocytes*. *Journal of Biological Chemistry*, **287**, 37134–37144.

Atkinson, A., Renziehausen, A., Wang, H., Lo Nigro, C., Lattanzio, L., Merlano, M., Rao, B., Weir, L., Evans, A., Matin, R., Harwood, C., Szlosarek, P., Pickering, J. G., Fleming, C., sim, V. R., Li, S., Vasta, J. T., Raines, R. T., Boniol, M., thompson, A., Proby, C., Crook, T. & Syed, N. (2019). Collagen Prolyl Hydroxylases Are Bifunctional Growth Regulators in Melanoma. *The Journal of Investigative Dermatology*, **139**, 1118–1126.

Attieh, Y., Clark, A. G., Grass, C., Richon, S., Pocard, M., Mariani, P., Elkhatib, N., Betz, T., Gurchenkov, B., & Vignjevic, D. M. (2017). Cancer-associated fibroblasts lead tumor invasion through integrin-β3-dependent fibronectin assembly. *The Journal of Cell Biology*, **216**, 3509–3520.

Bachmann, M., Kukkurainen, S., Hytönen, V. P., & Wehrle-Haller, B. (2019). Cell Adhesion by Integrins. *Physiological Reviews*, **99**, 1655–1699.

Balkwill, F. R., Capasso, M., & Hagemann, T. (2012). The tumor microenvironment at a glance. *Journal of Cell Science*, **125**, 5591–5596.

Barrett, R. L., & Puré, E. (2020). Cancer-associated fibroblasts and their influence on tumor immunity and immunotherapy. *ELife*, **9**, e57243.

Belhabib, I., Zaghdoudi, S., Lac, C., Bousquet, C., & Jean, C. (2021). Extracellular Matrices and Cancer-Associated Fibroblasts: Targets for Cancer Diagnosis and Therapy? *Cancers*, **13**, 3466.

Bhattacharya, S., Calar, K., & De La Puente, P. (2020). Mimicking tumor hypoxia and tumor-immune interactions employing three-dimensional in vitro models. *Journal of Experimental and Clinical Cancer Research*, **39**, 1–16.

Boucherit, N., Gorvel, L., & Olive, D. (2020). 3D Tumor Models and Their Use for the Testing of Immunotherapies. *Frontiers in Immunology*, **11**, 603640.

Boukamp, P., Stanbridge, E. J., Foo, D. Y., Cerutti, P. A., & Fusenig, N. E. (1990). c-Ha-ras oncogene expression in immortalized human keratinocytes (HaCaT) alters growth potential in vivo but lacks correlation with malignancy. *Cancer Research*, **50**, 2840–2847.

Bousquet, P. A., Sandvik, J. A., Arntzen, M. Ø., Jeppesen Edin, N. F., Christoffersen, S., Krengel, U., Pettersen, E. O., & Thiede, B. (2015). Hypoxia Strongly Affects Mitochondrial Ribosomal Proteins and Translocases, as Shown by Quantitative Proteomics of HeLa Cells. *International Journal of Proteomics*, **2015**, 678527.

Brassart-Pasco, S., Brézillon, S., Brassart, B., Ramont, L., Oudart, J. B., & Monboisse, J. C. (2020). Tumor Microenvironment: Extracellular Matrix Alterations Influence Tumor Progression. *Frontiers in Oncology*, **10**, 1–13.

Brinckmann, J., Açil, Y., Tronnier, M., Notbohm, H., Bätge, B., Schmeller, W., Koch, M. H., Müller, P. K., & Wolff, H. H. (1996). Altered x-ray diffraction pattern is accompanied by a change in the mode of cross-link formation in lipodermatosclerosis. *The Journal of Investigative Dermatology*, **107**, 589–592.

Burgeson, R. E. (1993). Type VII Collagen, Anchoring Fibrils, and Epidermolysis Bullosa. *Journal of Investigative Dermatology*, **101**, 252–255.

Calaluce, R., Kunkel, M. W., Watts, G. S., Schmelz, M., Hao, J., Barrera, J., Gleason-Guzman, M., Isett, R., Fitchmun, M., Bowden, G. T., Cress, A. E., Futscher, B. W., & Nagle, R. B. (2001). Laminin-5-mediated gene expression in human prostate carcinoma cells. *Molecular Carcinogenesis*, **30**, 119–129.

Chang, D., & Shain, A. H. (2021). The landscape of driver mutations in cutaneous squamous cell carcinoma. *Npj Genomic Medicine*, **6**, 61.

Chen, X., Zhang, S., Wang, Z., Wang, F., Cao, X., Wu, Q., Zhao, C., Ma, H., Ye, F., Wang, H., & Fang, Z. (2018). Supervillin promotes epithelial-mesenchymal transition and metastasis of hepatocellular carcinoma in hypoxia via activation of the RhoA/ROCK-ERK/p38 pathway. *Journal of Experimental & Clinical Cancer Research*, **37**, 128.

Clause, K. C., & Barker, T. H. (2013). Extracellular matrix signaling in morphogenesis and repair. *Current Opinion in Biotechnology*, **24**, 830–833.

Cloutier, G., Sallenbach-Morrissette, A., & Beaulieu, J.-F. (2019). Non-integrin laminin

receptors in epithelia. *Tissue and Cell*, **56**, 71–78.

Cox, T. R., & Erler, J. T. (2011). Remodeling and homeostasis of the extracellular matrix: implications for fibrotic diseases and cancer. *Disease Models & Mechanisms*, **4**, 165–178.

D'Arcangelo, E., Wu, N. C., Cadavid, J. L., & McGuigan, A. P. (2020). The life cycle of cancer-associated fibroblasts within the tumour stroma and its importance in disease outcome. *British Journal of Cancer*, **122**, 931–942.

Déry, M.-A. C., Michaud, M. D., & Richard, D. E. (2005). Hypoxia-inducible factor 1: regulation by hypoxic and non-hypoxic activators. *The International Journal of Biochemistry & Cell Biology*, **37**, 535–540.

Domogatskaya, A., Rodin, S., & Tryggvason, K. (2012). Functional diversity of laminins. *Annual Review of Cell and Developmental Biology*, **28**, 523–553.

Edmondson, R., Broglie, J. J., Adcock, A. F., & Yang, L. (2014). Three-dimensional cell culture systems and their applications in drug discovery and cell-based biosensors. *Assay and Drug Development Technologies*, **14**, 207–218.

Elango, J., Hou, C., Bao, B., Wang, S., de Val, J. E., & Wenhui, W. (2022). The Molecular Interaction of Collagen with Cell Receptors for Biological Function. *Polymers*, *14*.

Emami Nejad, A., Najafgholian, S., Rostami, A., Sistani, A., Shojaeifar, S., Esparvarinha, M., Nedaeinia, R., Haghjooy Javanmard, S., Taherian, M., Ahmadlou, M., Salehi, R., Sadeghi, B., & Manian, M. (2021). The role of hypoxia in the tumor microenvironment and development of cancer stem cell: a novel approach to developing treatment. *Cancer Cell International*, **21**, 62.

Eriksson, J., Le Joncour, V., Jahkola, T., Juteau, S., Laakkonen, P., Saksela, O., & Hölttä, E. (2020). Prolyl 4-hydroxylase subunit alpha 1 (P4HA1) is a biomarker of poor prognosis in primary melanomas, and its depletion inhibits melanoma cell invasion and disrupts tumor blood vessel walls. *Molecular Oncology*, **14**, 742–762.

Esco, M. A., Wang, Z., McDermott, M. L., & Kurpakus-Wheater, M. (2001). Potential role for laminin 5 in hypoxia-mediated apoptosis of human corneal epithelial cells. *Journal of Cell Science*, **114**, 4033–4040.

Fania, L., Didona, D., Di Pietro, F. R., Verkhovskaia, S., Morese, R., Paolino, G., Donati, M., Ricci, F., Coco, V., Ricci, F., Candi, E., Abeni, D., & Dellambra, E. (2021). Cutaneous Squamous Cell Carcinoma: From Pathophysiology to Novel Therapeutic Approaches. *Biomedicines*, **9**, 171.

Friedman, G., Levi-Galibov, O., David, E., Bornstein, C., Giladi, A., Dadiani, M., Mayo, A., Halperin, C., Pevsner-Fischer, M., Lavon, H., Mayer, S., Nevo, R., Stein, Y., Balint-Lahat, N., Barshack, I., Raza Ali, H, Caldas, C., Nili-Gal-Yam, E., Alon, U., Amit, I. & Scherz-Shouval, R. (2020). Cancer-associated fibroblast compositions change with breast cancer progression linking the ratio of S100A4+ and PDPN+ CAFs to clinical outcome. *Nature Cancer*, **1**, 692–708.

Furuta, C., Miyamoto, T., Takagi, T., Noguchi, Y., Kaneko, J., Itoh, S., Watanabe, T., & Itoh, F. (2015). Transforming growth factor-β signaling enhancement by long-term exposure to hypoxia in a tumor microenvironment composed of Lewis lung carcinoma cells. *Cancer Science*, **106**, 1524–1533.

Gagnoux-Palacios, L., Allegra, M., Spirito, F., Pommeret, O., Romero, C., Ortonne, J. P., & Meneguzzi, G. (2001). The short arm of the laminin gamma2 chain plays a pivotal role in the incorporation of laminin 5 into the extracellular matrix and in cell adhesion. *The Journal of Cell Biology*, **153**, 835–850.

Gilkes, D. M., Bajpai, S., Chaturvedi, P., Wirtz, D., & Semenza, G. L. (2013a). Hypoxia-inducible f0actor 1 (HIF-1) promotes extracellular matrix remodeling under hypoxic conditions by inducing P4HA1, P4HA2, and PLOD2 expression in fibroblasts. *Journal of Biological Chemistry*, **288**, 10819–10829.

Gilkes, D. M., Bajpai, S., Wong, C. C., Chaturvedi, P., Hubbi, M. E., Wirtz, D., & Semenza, G. L. (2013b). Procollagen lysyl hydroxylase 2 is essential for hypoxia-induced breast cancer metastasis. *Molecular Cancer Research : MCR*, **11**, 456–466.

Gilkes, D. M., Semenza, G. L., & Wirtz, D. (2014). Hypoxia and the extracellular matrix: drivers of tumour metastasis. *Nature Reviews. Cancer*, **14**, 430–439.

Guess, C. M., & Quaranta, V. (2009). Defining the role of laminin-332 in carcinoma. *Matrix Biology*, **28**, 445–455.

Halder, S. K., Kant, R., & Milner, R. (2018). Chronic mild hypoxia increases expression of laminins 111 and 411 and the laminin receptor α6β1 integrin at the blood-brain barrier. *Brain Research*, **1700**, 78–85.

Ham, S. L., Joshi, R., Luker, G. D., & Tavana, H. (2016). Engineered Breast Cancer Cell Spheroids Reproduce Biologic Properties of Solid Tumors. *Advanced Healthcare Materials*, **5**, 2788–2798.

He, Y., Jian, C. X., Zhang, H. Y., Zhou, Y., Wu, X., Zhang, G., & Tan, Y. H. (2016). Hypoxia enhances periodontal ligament stem cell proliferation via the MAPK

signaling pathway. *Genet Mol Res*, **15**, 10–4238.

Henke, E., Nandigama, R., & Ergün, S. (2020). Extracellular Matrix in the Tumor Microenvironment and Its Impact on Cancer Therapy. *Frontiers in Molecular Biosciences*, **6**, 160.

Hofbauer, K.-H., Gess, B., Lohaus, C., Meyer, H. E., Katschinski, D., & Kurtz, A. (2003). Oxygen tension regulates the expression of a group of procollagen hydroxylases. *European Journal of Biochemistry*, **270**, 4515–4522.

Humar, R., Kiefer, F. N., Berns, H., Resink, T. J., & Battegay, E. J. (2002). Hypoxia enhances vascular cell proliferation and angiogenesis in vitro via rapamycin (mTOR) -dependent signaling. *The FASEB Journal*, **16**, 771–780.

Jaakkola, P., Mole, D. R., Tian, Y. M., Wilson, M. I., Gielbert, J., Gaskell, S. J., von Kriegsheim, A., Hebestreit, H. F., Mukherji, M., Schofield, C. J., Maxwell, P. H., Pugh, C. W., & Ratcliffe, P. J. (2001). Targeting of HIF-alpha to the von Hippel-Lindau ubiquitylation complex by O2-regulated prolyl hydroxylation. *Science (New York, N.Y.)*, **292**, 468–472.

Junttila, M. R., Ala-aho, R., Jokilehto, T., Peltonen, J., Kallajoki, M., Grenman, R., Jaakkola, P., Westermarck, J., & Kähäri, V.-M. (2007). p38α and p38δ mitogen-activated protein kinase isoforms regulate invasion and growth of head and neck squamous carcinoma cells. *Oncogene*, **26**, 5267–5279.

Kalluri, R. (2016). The biology and function of fibroblasts in cancer. *Nature Reviews Cancer*, **16**, 582–598.

Kapałczyńska, M., Kolenda, T., Przybyła, W., Zajączkowska, M., Teresiak, A., Filas, V., Ibbs, M., Bliźniak, R., Łuczewski, Ł., & Lamperska, K. (2018). 2D and 3D cell cultures - a comparison of different types of cancer cell cultures. *Archives of Medical Science : AMS*, **14**, 910–919.

Karampoga, A., Tzaferi, K., Koutsakis, C., Kyriakopoulou, K., & Karamanos, N. (2022). Exosomes and the Extracellular Matrix: a dynamic interplay in cancer progression. *The International Journal of Developmental Biology*, **66**, 97–102.

Katayama, M., & Sekiguchi, K. (2004). Laminin-5 in Epithelial Tumour Invasion. *Journal of Molecular Histology*, **35**, 277–286.

Khoshnoodi, J., Pedchenko, V., & Hudson, B. G. (2008). Mammalian collagen IV. *Microscopy Research and Technique*, **71**, 357–370.

Kim, H., Lin, Q., Glazer, P. M., & Yun, Z. (2018). The hypoxic tumor microenvironment

in vivo selects the cancer stem cell fate of breast cancer cells. *Breast Cancer Research*, **20**, 16.

Kim, J. Y. S., Kozlow, J. H., Mittal, B., Moyer, J., Olenecki, T., & Rodgers, P. (2018). Guidelines of care for the management of cutaneous squamous cell carcinoma. *Journal of the American Academy of Dermatology*, **78**, 560–578.

Kim, Y. E., Jeon, H. J., Kim, D., Lee, S. Y., Kim, K. Y., Hong, J., Maeng, P. J., Kim, K.-R., & Kang, D. (2018). Quantitative Proteomic Analysis of 2D and 3D Cultured Colorectal Cancer Cells: Profiling of Tankyrase Inhibitor XAV939-Induced Proteome. *Scientific Reports*, **8**, 13255.

King, R., Hayes, C., Donohoe, C. L., Dunne, M. R., Davern, M., & Donlon, N. E. (2021). Hypoxia and its impact on the tumour microenvironment of gastroesophageal cancers. *World Journal of Gastrointestinal Oncology*, **13**, 312–331.

Kirtonia, A., Pandey, A. K., Ramachandran, B., Mishra, D. P., Dawson, D. W., Sethi, G., Ganesan, T. S., Koeffler, H. P., & Garg, M. (2022). Overexpression of laminin-5 gamma-2 promotes tumorigenesis of pancreatic ductal adenocarcinoma through EGFR/ERK1/2/AKT/mTOR cascade. *Cellular and Molecular Life Sciences*, **79**, 362.

Kučera, J., Netušilová, J., Sladeček, S., Lánová, M., Vašíček, O., Štefková, K., Navrátilová, J., Kubala, L., & Pacherník, J. (2017). Hypoxia Downregulates MAPK/ERK but Not STAT3 Signaling in ROS-Dependent and HIF-1-Independent Manners in Mouse Embryonic Stem Cells. *Oxidative Medicine and Cellular Longevity*, **2017**, 4386947.

Kusindarta, D. L., & Wihadmadyatami, H. (2018). The Role of Extracellular Matrix in Tissue Regeneration. *Tissue Regeneration*. **65**

Kwon, S. Y., Chun, S. Y., Ha, Y.-S., Kim, D. H., Kim, J., Song, P. H., Kim, H. T., Yoo, E. S., Kim, B. S., & Kwon, T. G. (2017). Hypoxia Enhances Cell Properties of Human Mesenchymal Stem Cells. *Tissue Engineering and Regenerative Medicine*, **14**, 595–604.

LeBleu, V. S., & Kalluri, R. (2018). A peek into cancer-associated fibroblasts: origins, functions and translational impact. *Disease Models & Mechanisms*, **11**, dmm029447.

Levental, K. R., Yu, H., Kass, L., Lakins, J. N., Egeblad, M., Erler, J. T., Fong, S. F. T., Csiszar, K., Giaccia, A., Weninger, W., Yamauchi, M., Gasser, D. L., & Weaver, V.

M. (2009). Matrix crosslinking forces tumor progression by enhancing integrin signaling. *Cell*, **139**, 891–906.

Li, Teixeira, A. F., Zhu, H.-J., & Ten Dijke, P. (2021). Cancer associated-fibroblast-derived exosomes in cancer progression. *Molecular Cancer*, **20**, 154.

Li, Y., Ge, Y. Z., Qian, Y., Chen, K., Zhao, F., Qin, Z., Zhou, L., Xu, L., Xu, Z., Dou, Q., & Jia, R. (2022). The Role of P4HA1 in Multiple Cancer Types and its Potential as a Target in Renal Cell Carcinoma. *Frontiers in Genetics*, **13**, 1–15.

Lin, S.-C., Liao, W.-L., Lee, J.-C., & Tsai, S.-J. (2014). Hypoxia-regulated gene network in drug resistance and cancer progression. *Experimental Biology and Medicine (Maywood, N.J.)*, **239**.

Liu, B., Liu, T., Liu, Y., Feng, X., Jiang, X., Long, J., Ye, S., Chen, D., Wang, J., & Yang, Z. (2022). TSG-6 promotes Cancer Cell aggressiveness in a CD44-Dependent Manner and Reprograms Normal Fibroblasts to create a Pro-metastatic Microenvironment in Colorectal Cancer. *International Journal of Biological Sciences*, **18**, 1677–1694.

Lohi, J., Oivula, J., Kivilaakso, E., Kiviluoto, T., Fröjdman, K., Yamada, Y., Burgeson, R. E., Leivo, I., & Virtanen, I. (2000). Basement membrane laminin-5 is deposited in colorectal adenomas and carcinomas and serves as a ligand for alpha3beta1 integrin. *APMIS : Acta Pathologica, Microbiologica, et Immunologica Scandinavica*, **108**, 161–172.

Lu, P., Takai, K., Weaver, V. M., & Werb, Z. (2011). Extracellular matrix degradation and remodeling in development and disease. *Cold Spring Harbor Perspectives in Biology*, **3**, a005058.

Mallikarjuna, P., Zhou, Y., & Landström, M. (2022). The Synergistic Cooperation between TGF-β and Hypoxia in Cancer and Fibrosis. *Biomolecules*, **12**, 635.

Marinkovich, M. P. (2007). Laminin 332 in squamous-cell carcinoma. *Nature Reviews Cancer*, **7**, 370–380.

Martins, C., Ana, C., Dâmaso, S., Casimiro, S., & Costa, L. (2020). Collagen biology making inroads into prognosis and treatment of cancer progression and metastasis. *Cancer and Metastasis Reviews*, **39**, 603–623.

Mhaidly, R., & Mechta-Grigoriou, F. (2020). Fibroblast heterogeneity in tumor micro-environment: Role in immunosuppression and new therapies. *Seminars in Immunology*, **48**, 101417.

Mizushima, H., Hirosaki, T., Miyata, S., Takamura, H., Miyagi, Y., & Miyazaki, K. (2002). Expression of laminin-5 enhances tumorigenicity of human fibrosarcoma cells in nude mice. *Japanese Journal of Cancer Research*, **93**, 652–659.

Mohan, P. S., Chou, D. K. H., & Jungalwala, F. B. (1990). Sulfoglucuronyl Glycolipids Bind Laminin. *Journal of Neurochemistry*, **54**, 2024–2031.

Muz, B., de la Puente, P., Azab, F., & Azab, A. K. (2015). The role of hypoxia in cancer progression, angiogenesis, metastasis, and resistance to therapy. *Hypoxia (Auckland, N.Z.)*, **3**, 83–92.

Myllyharju, J., & Kivirikko, K. I. (2004). Collagens, modifying enzymes and their mutations in humans, flies and worms. *Trends in Genetics : TIG*, **20**, 33–43.

Myllyharju, J., & Schipani, E. (2010). Extracellular matrix genes as hypoxia-inducible targets. *Cell and Tissue Research*, **339**, 19–29.

Nishida, N., Yano, H., Nishida, T., Kamura, T., & Kojiro, M. (2006). Angiogenesis in cancer. *Vascular Health and Risk Management*, **2**, 213–219.

O'Toole, E. A., Marinkovich, M. P., Peavey, C. L., Amieva, M. R., Furthmayr, H., Mustoe, T. A., & Woodley, D. T. (1997). Hypoxia increases human keratinocyte motility on connective tissue. *Journal of Clinical Investigation*, **100**, 2881–2891.

Ojalill, M., Parikainen, M., Rappu, P., Aalto, E., Jokinen, J., Virtanen, N., Siljamäki, E., & Heino, J. (2018). Integrin α2β1 decelerates proliferation, but promotes survival and invasion of prostate cancer cells. *Oncotarget*, **9**, 32435–32447.

Ojalill, M., Virtanen, N., Rappu, P., Siljamäki, E., Taimen, P., & Heino, J. (2020). Interaction between prostate cancer cells and prostate fibroblasts promotes accumulation and proteolytic processing of basement membrane proteins. *Prostate*, **80**, 715–726.

Paradisi, A., Waterboer, T., Ricci, F., Sampogna, F., Pawlita, M., & Abeni, D. (2020). Concomitant seropositivity for HPV 16 and cutaneous HPV types increases the risk of recurrent squamous cell carcinoma of the skin. *European Journal of Dermatology*, **30**, 493–498.

Peirsman, A., Blondeel, E., Ahmed, T., Anckaert, J., Audenaert, D., Boterberg, T., Buzas, K., Carragher, N., Castellani, G., Castro, F., Dangles-Marie, V., Dawson, J., De Tullio, J., De Vlieghere, E., Dedeyne, S., Depypere, H., Diosdi, A., I. Dmitriev, R., Dolznig, H., Fischer, S., Gespach, C., Goossens, V., Heino, J., Hendrix, A., Horvath, P., Kunz-Schughart, L. A., Maes, S., Mangodt, C., Mestdagh, P., Michlíková, S.,

Olivera, M. J., Pampaloni, F., Piccinini, F., Pinheiro, C., Rahn, J., Robbins, S. M., Siljamäki, E., Steigemann, P., Sys, G., Takayama, S., Tesei, A., Tulkens, J., Waeyenberge, M. V., Vandesompele, J., Wagemans, G., Weindorfer, C., Yigit, N., Zablowsky, N., Zanoni, M., Blondeel, P. & De Wever, O. (2021). MISpheroID: a knowledgebase and transparency tool for minimum information in spheroid identity. *Nature Methods*, **18**, 1294–1303.

Petrova, V., Annicchiarico-Petruzzelli, M., Melino, G., & Amelio, I. (2018). The hypoxic tumour microenvironment. *Oncogenesis*, **7**, 10.

Pinnel, S. R., Murad, S., & Darr, D. (1987). Induction of collagen synthesis by ascorbic acid. A possible mechanism. *Archives of Dermatology*, **123**, 1684–1686.

Pinnell, S. R. (1985). Regulation of collagen biosynthesis by ascorbic acid: A review. *Yale Journal of Biology and Medicine*, **58**, 553–559.

Powell, C. S., Wright, M. M., & Jackson, R. M. (2004). p38mapk and MEK1/2 inhibition contribute to cellular oxidant injury after hypoxia. *American Journal of Physiology-Lung Cellular and Molecular Physiology*, **286**, 826–833.

Provenzano, P. P., Eliceiri, K. W., & Keely, P. J. (2009). Multiphoton microscopy and fluorescence lifetime imaging microscopy (FLIM) to monitor metastasis and the tumor microenvironment. *Clinical & Experimental Metastasis*, **26**, 357–370.

Prudovsky, I. (2021). Cellular Mechanisms of FGF-Stimulated Tissue Repair. *Cells*, *10*.

Qi, Y., & Xu, R. (2018). Roles of PLODs in Collagen Synthesis and Cancer Progression. *Frontiers in Cell and Developmental Biology*, **6**, 66.

Qiu, Y., Li, P., & Ji, C. (2015). Cell Death Conversion under Hypoxic Condition in Tumor Development and Therapy. *International Journal of Molecular Sciences*, **16**, 25536–25551.

Rappu, P., Salo, A. M., Myllyharju, J., & Heino, J. (2019). Role of prolyl hydroxylation in the molecular interactions of collagens. *Essays In Biochemistry*, **63**, EBC20180053.

Ricard-Blum, S. (2011). The collagen family. *Cold Spring Harbor Perspectives in Biology*, **3**, a004978.

Riffle, S., & Hegde, R. S. (2017). Modeling tumor cell adaptations to hypoxia in multicellular tumor spheroids. *Journal of Experimental and Clinical Cancer Research*, **36**, 102.

Robinson, A. D., Chakravarthi, B. V. S. K., Agarwal, S., Chandrashekar, D. S.,

Davenport, M. L., Chen, G., Manne, U., Beer, D. G., Edmonds, M. D., & Varambally, S. (2021). Collagen modifying enzyme P4HA1 is overexpressed and plays a role in lung adenocarcinoma. *Translational Oncology*, **14**, 101128.

Rousselle, P., & Scoazec, J. Y. (2020). Laminin 332 in cancer: When the extracellular matrix turns signals from cell anchorage to cell movement. *Seminars in Cancer Biology*, **62**, 149–165.

Schlie-Wolter, S., Ngezahayo, A., & Chichkov, B. N. (2013). The selective role of ECM components on cell adhesion, morphology, proliferation and communication in vitro. *Experimental Cell Research*, **319**, 1553–1561.

Shoulders, M. D., & Raines, R. T. (2009). Collagen structure and stability. *Annual Review of Biochemistry*, **78**, 929–958.

Siljamäki, E, Riihilä, P., Suwal, U., Nissinen, L., Rappu, P., Kallajoki, M., Kähäri, V.-M., & Heino, J. (2022). PLX8394, an oral serine-threonine kinase inhibitor, prevents TGF-β induced laminin-332 synthesis, cell invasion and tumor growth in cutaneous squamous cell carcinoma. *Manuscript in preparation.*

Siljamäki, E., Rappu, P., Riihilä, P., Nissinen, L., Kähäri, V.-M., & Heino, J. (2020). H-Ras activation and fibroblast-associated TGF-β signaling promote laminin-332 accumulation and invasion in cutaneous squamous cell carcinoma. *Matrix Biology*, **87**, 26–47.

Stegen, S., Laperre, K., Eelen, G., Rinaldi, G., Fraisl, P., Torrekens, S., … Carmeliet, G. (2019). HIF-1α metabolically controls collagen synthesis and modification in chondrocytes. *Nature*, **565**, 511–515.

Stratigos, A. J., Garbe, C., Dessinioti, C., Lebbe, C., Bataille, V., Bastholt, L., … Grob, J.-J. (2020). European interdisciplinary guideline on invasive squamous cell carcinoma of the skin: Part 1. epidemiology, diagnostics and prevention. *European Journal of Cancer (Oxford, England : 1990)*, **128**, 60–82.

Sun, X., Wei, L., Chen, Q., & Terek, R. M. (2010). CXCR4/SDF1 mediate hypoxia induced chondrosarcoma cell invasion through ERK signaling and increased MMP1 expression. *Molecular Cancer*, **9**, 17.

Tripathi, M., Nandana, S., Yamashita, H., Ganesan, R., Kirchhofer, D., & Quaranta, V. (2008). Laminin-332 is a substrate for hepsin, a protease associated with prostate cancer progression. *Journal of Biological Chemistry*, **283**, 30576–30584.

Turck, N., Gross, I., Gendry, P., Stutzmann, J., Freund, J.-N., Kedinger, M., Simon-

Assmann, P., & Launay, J.-F. (2005). Laminin isoforms: biological roles and effects on the intracellular distribution of nuclear proteins in intestinal epithelial cells. *Experimental Cell Research*, **303**, 494–503.

Vaapil, M., Helczynska, K., Villadsen, R., Petersen, O. W., Johansson, E., Beckman, S., Larsson, C., Påhlman, S., & Jögi, A. (2012). Hypoxic conditions induce a cancer-like phenotype in human breast epithelial cells. *PloS One*, **7**, e46543.

Vinaiphat, A., Low, J. K., Yeoh, K. W., Chng, W. J., & Sze, S. K. (2021). Application of Advanced Mass Spectrometry-Based Proteomics to Study Hypoxia Driven Cancer Progression. *Frontiers in Oncology*, **11**, 98.

Walker, C., Mojares, E., & Del Río Hernández, A. (2018). Role of Extracellular Matrix in Development and Cancer Progression. *International Journal of Molecular Sciences*, **19**, 3028.

Wu, J., Reinhardt, D. P., Batmunkh, C., Lindenmaier, W., Far, R. K.-K., Notbohm, H., Hunzelmann, N., & Brinckmann, J. (2006). Functional diversity of lysyl hydroxylase 2 in collagen synthesis of human dermal fibroblasts. *Experimental Cell Research*, **312**, 3485–3494.

Xiao, Q., & Ge, G. (2012). Lysyl oxidase, extracellular matrix remodeling and cancer metastasis. *Cancer Microenvironment : Official Journal of the International Cancer Microenvironment Society*, **5**, 261–273.

Xiong, G., Deng, L., Zhu, J., Rychahou, P. G., & Xu, R. (2014). Prolyl-4-hydroxylase α subunit 2 promotes breast cancer progression and metastasis by regulating collagen deposition. *BMC Cancer*, **14**, 1.

Xiong, G., Stewart, R. L., Chen, J., Gao, T., Scott, T. L., Samayoa, L. M., O'Connor, K., Lane, A. N., & Xu, R. (2018). Collagen prolyl 4-hydroxylase 1 is essential for HIF-1α stabilization and TNBC chemoresistance. *Nature Communications*, **9**, 4456.

Xu, S., Xu, H., Wang, W., Li, S., Li, H., Li, T., Zhang, W., Yu, X., & Liu, L. (2019). The role of collagen in cancer: From bench to bedside. *Journal of Translational Medicine*, **17**, 1–22.

Yamamoto, H., Itoh, F., Iku, S., Hosokawa, M., & Imai, K. (2001). Expression of the gamma(2) chain of laminin-5 at the invasive front is associated with recurrence and poor prognosis in human esophageal squamous cell carcinoma. *Clinical Cancer Research : An Official Journal of the American Association for Cancer Research*, **7**, 896–900.

Yang, Y., Li, Y., Qi, R., & Zhang, L. (2021). Constructe a novel 5 hypoxia genes signature for cervical cancer. *Cancer Cell International*, **21**, 345.

Yeowell, H. N., Walker, L. C., Murad, S., & Pinnell, S. R. (1997). A common duplication in the lysyl hydroxylase gene of patients with Ehlers Danlos syndrome type VI results in preferential stimulation of lysyl hydroxylase activity and mRNA by hydralazine. *Archives of Biochemistry and Biophysics*, **347**, 126–131.

Yurchenco, P. D. (2011). Basement membranes: cell scaffoldings and signaling platforms. *Cold Spring Harbor Perspectives in Biology*, **3**, a004911.

Zhang, Q., Yin, Y., Zhao, H., Shi, Y., Zhang, W., Yang, Z., Liu, T., Huang, Y., & Yu, Z. (2021). P4HA1 regulates human colorectal cancer cells through HIF1α-mediated Wnt signaling. *Oncology Letters*, **21**, 145.

Zhao, Q., & Liu, J. (2021). P4HA1, a Prognostic Biomarker that Correlates With Immune Infiltrates in Lung Adenocarcinoma and Pan-Cancer. *Frontiers in Cell and Developmental Biology*, **9**, 754580.

Zhou, H., Wu, G., Ma, X., Xiao, J., Yu, G., Yang, C., Xu, N., Zhang, B., Zhou, J., Ye, Z., & Wang, Z. (2018). Attenuation of TGFBR2 expression and tumour progression in prostate cancer involve diverse hypoxia-regulated pathways. *Journal of Experimental & Clinical Cancer Research*, **37**, 89.

Zhu, C., Yu, J., Pan, Q., Yang, J., Hao, G., Wang, Y., Li, L., & Cao, H. (2016). Hypoxia-inducible factor-2 alpha promotes the proliferation of human placenta-derived mesenchymal stem cells through the MAPK/ERK signaling pathway. *Scientific Reports*, **6**, 35489.

Ziello, J. E., Jovin, I. S., & Huang, Y. (2007). Hypoxia-Inducible Factor (HIF)-1 regulatory pathway and its potential for therapeutic intervention in malignancy and ischemia. *The Yale Journal of Biology and Medicine*, **80**, 51–60.